Isotope discrimination of carbonyl sulfide (34S) and carbon dioxide (13C, 18O) during plant uptake in flow-through chamber experiments

Sophie L. Baartman^{1,2}, Steven M. Driever³, Maarten Wassenaar⁴, Linda M.J. Kooijmans², Nerea Ubierna⁶, Leon Mossink³, Maria E. Popa², Ara Cho², Lisa Wingate⁶, Thomas Röckmann¹,

Steven M.A.C. van Heuven⁵, Maarten C. Krol^{1,2}

¹Institute for Marine and Atmospheric Research Utrecht (IMAU), Princetonplein 5, 3584 CC Utrecht, The Netherlands

²Meteorology and Air Quality, Wageningen University and Research Centre, Droevendaalsesteeg 4, 6708 PB Wageningen, The Netherlands

³Centre for Crop Systems Analysis, Wageningen University and Research Centre, Droevendaalsesteeg 4, 6708 PB Wageningen, The Netherlands

⁴Horticulture and Product Physiology, Wageningen University and Research Centre, Droevendaalsesteeg 4, 6708 PB Wageningen, The Netherlands

15 Scentre for Isotope Research (CIO), Energy and Sustainability Research Institute Groningen, University of Groningen, 9747 AG Groningen, the Netherlands

⁶Institut National de la Recherche Agronomique, Bordeaux Sciences Agro, Unité Mixte de Recherche 1391, Interactions Sol-Plante-Atmosphère, 33140 Villenave d'Ornon, France

Correspondence to: Sophie L. Baartman (sophie.baartman@wur.nl)

20

25

35

Abstract. Carbonyl sulfide (COS) has been proposed as a proxy for gross primary production (GPP), as it is taken up by plants through a pathway comparable to that of CO₂. COS diffuses into the leaf, where it undergoes an essentially one-way reaction in the mesophyll cells, catalyzed by the enzyme carbonic anhydrase (CA), and is likely not respired by the leaf. In order to use COS as a proxy for GPP, the mechanisms of COS uptake and its coupling to photosynthesis need to be well understood. Characterizing the isotopic discrimination of COS during plant uptake could provide valuable information on the physiological COS uptake process and may help to constrain the COS budget.

This study presents joint measurements of isotope discrimination during plant uptake for COS (CO³⁴S) and CO₂ (I³CO₂ and C¹⁸O¹⁶O). A C₃ plant, sunflower (*Helianthus annuus*), and a C₄ plant, papyrus (*Cyperus papyrus*), were enclosed in a flow-through plant chamber and exposed to varying light levels. The incoming and outgoing gas compositions were measured online, and discrete air samples were taken for isotope analysis. Simultaneously measuring fluxes and isotope discrimination of both COS and CO₂ yielded a unique dataset that includes information on the plant's behavior and allowed for the estimation of stomatal- and mesophyll conductance.

The average COS uptake fluxes were 73.3 ± 1.5 pmol m⁻² s⁻¹ for sunflower and 107.3 ± 1.5 pmol m⁻² s⁻¹ for papyrus (PAR > 0) and displayed virtually no trend with increasing PAR from 200 to 600 μ mol m⁻² s⁻¹. The mean observed ³⁴ Δ for COS was 3.4 ± 1.0 for sunflower and 2.6 ± 1.0 for papyrus. $\frac{34}{\Delta}$ was stable across all light

Deleted: Lopez

Deleted: comparable pathway as

Deleted: and

Deleted: does not exit the leaf

Deleted: again

Deleted: , however

Deleted: CO₂ uptake

Deleted: can

Deleted: useful

Deleted: can

Deleted: was

Deleted: around

Deleted: pmol mol-1

Deleted: between 99 and 110

Deleted: pmol mol-1

Deleted: corresponding

Deleted: 0.8

Deleted: 0.3

1

intensities, which could be explained by a sufficient stomatal opening and low variability in the ratio of mesophyll vs. ambient COS mole fraction, C_m^S/C_a^S . For CO₂, a negative relationship was observed between the uptake flux and the isotopic discriminations ¹³ Δ and ¹⁸ Δ . The CO₂ uptake and ¹³ Δ and ¹⁸ Δ values indicate that the sunflower behaved as expected for a C₃ plant, while the low CO₂ flux and high ¹³ Δ and ¹⁸ Δ values observed for papyrus were not in the typical C₄ range, which was perhaps due to the relatively low light conditions during our experiments.

Deleted: ∆

Deleted: our

Deleted: was not displaying

Deleted: behavior

1. Introduction

55

60

65

70

75

80

85

Photosynthetic uptake of carbon dioxide (CO2) by the terrestrial biosphere, quantified by the gross primary production (GPP), is the largest sink of atmospheric CO2, and may be altered as the climate changes (Friedlingstein et al., 2023). For making accurate future climate projections, it is important to quantify changes in the functioning of the biosphere and its influence on the atmospheric composition. Several techniques can be used to quantify photosynthesis and respiration fluxes at the ecosystem and larger scales, such as Eddy Covariance (EC) (Asaf et al., 2013; Billesbach et al., 2014; Commane et al., 2015; Wehr et al., 2017; Vesala et al., 2022) or variations in the stable isotopic composition of CO2 (e.g. Farquhar and Lloyd, 1993; Farquhar et al., 1993; Wingate et al., 2007; Gentsch et al., 2014; Wehr et al., 2015;). However, these techniques have limitations, because they either measure net CO2 fluxes (Wohlfahrt et al., 2012; Kooijmans et al., 2017) or they require additional measurements such as the oxygen isotopic composition of water pools (Wingate et al., 2010; Adnew et al., 2020). Because of these limitations, other potential independent proxies for GPP have recently gained attention, especially the trace gas carbonyl sulfide (COS or OCS, COS henceforth) (Sandoval-Soto et al., 2005; Montzka et al., 2007; Campbell et al., 2008; Whelan et al., 2018; Lai et al., 2024).

Deleted: e

Deleted: ppt

COS is the most abundant sulfur-containing atmospheric trace gas, with a tropospheric mole fraction of around 500 pmol mol⁻¹ that displays a strong seasonal cycle, mostly due to the uptake of COS by terrestrial vegetation during photosynthesis. Figure 1 shows a schematic of the uptake pathways and assimilation locations of COS and CO₂ in the leaf. Similarly to CO₂, COS diffuses across the leaf boundary layer, through the stomata and into the leaf mesophyll cells (Protoschill-Krebs and Kesselmeier, 1992; Protoschill-Krebs et al., 1996). There, COS is hydrolyzed in an essentially one-way reaction, catalyzed by the enzyme carbonic anhydrase (CA), in contrast to the reversible hydration reaction that CO₂ undergoes (Protoschill-Krebs and Kesselmeier, 1992; Protoschill-Krebs et al., 1996). Assuming that there is no COS emission, the COS uptake by plants is proportional to photosynthetic uptake of CO₂, and therefore, GPP can be derived from the leaf-scale relative uptake ratio (LRU) of COS and CO₂ uptake fluxes, A^S (pmol mol⁻² s⁻¹) and A^C (µmol mol⁻² s⁻¹), normalized to their atmospheric mole fractions, C_a^S (pmol mol⁻¹) and C_a^C (µmol mol⁻¹) using Eq. (1):

Deleted:

Formatted: Font: Not Italic

Deleted:

 $LRU = \frac{A^S}{A^C} * \frac{C_a^C}{C_s^S} \tag{1}$

If we assume negligible daytime leaf respiration, or if we account for it, A^{C} can be replaced by GPP, which can then be estimated using Eq. (2) (re-arrangement of Eq. (1)) (Campbell et al., 2008).

$$GPP = A^S \frac{C_a^C}{C_s^S} * \frac{1}{LRU}$$
 (2)

While the use of LRU as a link between COS and CO₂ fluxes seems promising, some studies have shown that the LRU is not constant among species and changes with environmental conditions such as photosynthetically active radiation (PAR), temperature and vapor pressure deficit (VPD) (Kooijmans et al., 2019; Maignan et al., 2021; Sun et al., 2022; Spielmann et al., 2023; Sun et al., 2024). Additionally, the existence of a COS compensation point suggests that emissions can occur for some species under certain circumstances (Goldan et al., 1988; Kesselmeier and Merk, 1993; Kuhn and Kesselmeier, 2000; Maseyk et al., 2014; Belviso et al., 2022) Thus, a more thorough understanding of the physiological drivers and limitations of COS uptake by plants, and its relationship with CO₂ uptake, is needed.

100

105

110

115

120

125

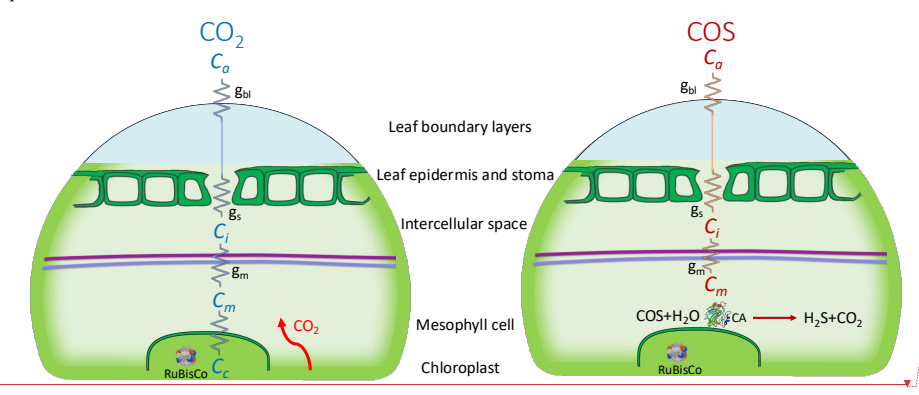


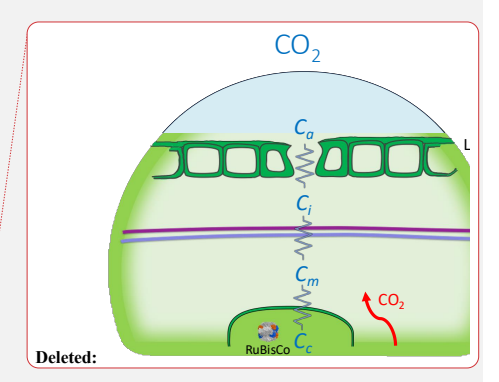
Figure 1. Schematic (simplified) representation of the diffusion pathways (zigzag lines) of CO2 (left) and COS (right) into a C3 leaf, with the conductance parameters being boundary layer- (gbi), stomatal- (gs) and mesophyll conductance (gm). The CO2 and COS mole fractions are indicated as Ca (atmospheric), Ci (intercellular space), Cm (mesophyll cell), and, for CO2, Cc indicates the mole fraction in the chloroplast (the green, bordered area), The enzymes ribulose-1,5-biphosphate, carboxylase oxygenase (RuBisCo, inside the chloroplast) and carbonic anhydrase (CA, right figure only) catalyze CO2 and COS fixation. The purple line represents the mesophyll cell wall, and the blue line indicates the plasma membrane.

Using the distinct fingerprints of chemical and diffusion processes, the isotopic fractionation of COS during plant uptake could be used to help improve understanding of processes driving COS plant uptake. For example, isotope measurements may provide insights on the role of environmental factors, such as PAR and VPD with respect to LRU variations. Improved global estimates of isotope discrimination of C₃ and C₄ species may then be used to better constrain the COS budget (Davidson et al., 2022) and possibly aid in improving the COS-derived GPP estimate.

Isotope studies on COS uptake build on the extensive experience and literature on the isotope effects associated with the uptake of CO₂. The discrimination against CO³⁴S (‰) is defined in Eq. (3), where ³²k and ³⁴k are the reaction rate coefficients for uptake of CO³²S and CO³⁴S, respectively:

$$^{34}\Delta = 1 - \frac{^{34}k}{^{32}k}. (3)$$

Isotope discrimination occurs both during diffusion of COS into the leaf and due to the preferential hydrolysis of lighter isotopologues by CA (Davidson et al., 2022). Similar to the model developed by Farquhar et al. (1982) for ¹³CO₂ discrimination during photosynthesis and as the reaction with CA is supposed to be irreversible (Protoschill-



Deleted:

 $\begin{tabular}{ll} \textbf{Deleted:} including the mole fractions of both species in the atmosphere (...$

Deleted:

Deleted: the intercellular space (

Deleted:)

Deleted: the mesophyll cell (

Deleted:)

Deleted: , the chloroplast (

Deleted:)

Deleted:

Deleted: fosfaat

Deleted: COS isotope discrimination during plant uptake could provide useful information on the uptake process and its response to environmental factors.

Deleted:

Formatted: English (UK)

155

160

165

170

175

180

<u>Krebs and Kesselmeier, 1992; Protoschill-Krebs et al., 1996)</u>, the net $CO^{34}S$ discrimination during plant uptake $(^{34}\Delta)$ can be expressed as a function of the ratio of COS mole fraction at the site of assimilation (the end-point), in the mesophyll cell (C_a^S) versus the COS mole fraction in ambient air (C_a^S) (Davidson et al., 2022):

$$^{34}\Delta = a + (h - a)\frac{c_m^S}{c_a^S},\tag{4}$$

where α is the fractionation occurring during diffusion of COS into the leaf up to the mesophyll cell, which incorporates leaf boundary layer (BL) diffusion, stomatal diffusion and gas-liquid interface dissolution and diffusion, and h is the S isotope fractionation during fixation by the enzyme carbonic anhydrase (CA).

 C_m^S has been suggested to be close to zero in C₃ plants (Stimler et al., 2011; Stimler et al., 2012). When C_m^S = 0_{∞} Eq. (4) reduces to $^{34}\Delta = \alpha$, thus $^{34}\Delta$ is caused solely by diffusion differences between CO³²S and CO³⁴S (α) through the stomata and up to the mesophyll. Binary molecular diffusion of COS in air is theoretically expected to provide a $^{34}\Delta$ value of around 5 ‰, because of the differences in molecular masses between the different COS isotopologues (Angert et al. 2019). However, this may be a too crude simplification of the diffusion processes taking place, as COS diffusion not only involves gaseous diffusion but also gas-liquid interface diffusion from the intercellular space to the mesophyll cell (Fig. 1) (Stimler et al., 2010; Berry et al., 2013). When including stomatal diffusion, leaf BL diffusion, and gas-liquid phase diffusion in the mesophyll cell, Davidson et al. (2022) calculated an overall diffusion fractionation value of $\alpha = 1.6 \pm 0.1$ ‰ for 34 S.

Still, it is not known whether the COS mole fraction in the mesophyll always reaches values close to zero, especially for C₄ species, in which CA activity is low₆(Stimler et al., 2011). In the case of non-zero C_{nm}^S values for the enzymatic fractionation during COS fixation by CA (h) are needed to calculate ³⁴ Δ . Davidson et al. (2022) determined an enzymatic fractionation for ³⁴S, h, of 15 ± 2 % from experiments in which the plants were exposed to high CO₂ (2900 ± 90 pmol mol⁻¹) and COS (3.4 ± 0.1 µmol mol⁻¹) mole fractions.

In another set of experiments by Davidson et al. (2022), this time using ambient CO₂ ($500 \pm 80 \text{ pmol mol}^{-1}$) and COS ($0.53 \pm 0.02 \text{ nmol mol}^{-1}$) mole fractions, their observed $^{34}\Delta$ values were $1.6 \pm 0.1 \%$ for C₃ and $5.4 \pm 0.5 \%$ for C₄ species. These authors attributed the higher discrimination value for C₄ species to the lower CA activity, which could lead to a non-zero COS mole fraction at the site of CA and discrimination by this enzyme.

As the methodology for isotope ratio measurements of COS has only recently been established (Hattori et al., 2015; Angert et al., 2019; Baartman et al., 2022), the only studies that have determine COS isotope discrimination during plant uptake are by Davidson et al., (2021) and Davidson et al., (2022). These studies used a closed-chamber approach and as mole fractions of CO₂, COS and H₂O change during experiments with closed chambers, there is a potential risk that feedback processes on stomatal conductance and other metabolic processes may have contributed to the observed discrimination. Hence, these results may not reflect typical leaf conditions. With flow-through chambers, conditions can be monitored online and kept stable throughout the entire experiment, also allowing for easier repetition of the experiments.

In this work, we introduce a new methodoly for measuring COS isotope discrimination in plants, using a flow-through plant chamber, which was closely monitored to maintain stable conditions. We demonstrate the advantages of simultaneously measuring COS and CO₂ fluxes, and isotope discrimination of COS uptake against CO³⁴S and CO₂ uptake against ¹³CO₂ and C¹²O¹⁸O (³⁴A, ¹³A, and ¹⁸A) in C₃ and C₄ species and at a range of PAR. Photosynthetic

Deleted:

Deleted:

Deleted: er

Deleted: is case

Deleted: The

Deleted:, measured in C₃ and C₄ species by Davidson et al. (2022), during their series of closed-chamber experiments,

Deleted:, respectively, at ambient COS and CO₂ mole fractions....

Deleted: Here, t

Deleted: likely reflects

Deleted: ing

Deleted: higher c_m and therefore an influence of b on the observed discrimination.

Deleted: To date,

Deleted: are the only studies that have determined COS isotope discrimination during plant uptake,

Deleted: and they used a closed-chamber approach. A

Deleted: and

Deleted: and hence

Deleted: ed

Deleted: ers

Deleted: , to perform joint measurements of

Deleted: and

Deleted: We determined the isotope discrimination of COS uptake against CO 3 4S and CO $_2$ uptake against 13 CO $_2$ and 12 O 18 O $(^{34}$ Δ , 13 Δ , and 18 Δ).

discrimination against ¹³CO₂ (¹³Δ) can be used to explain variations in photosynthesis rates and to estimate stomatal conductance (Farquhar & Richards, 1984; Farquhar et al., 1989; Cernusak et al., 2013). During photosynthesis, CO₂ can exchange oxygen atoms with the leaf water, catalyzed by CA, and partly diffuse back to the atmosphere with changed isotopic composition. The resulting apparent discrimination against ¹²C¹⁶O¹⁸O (¹⁸Δ) during photosynthesis can serve as a proxy for gross biosphere-atmosphere CO₂ exchange (Francey and Tans; Yakir, 1998; Adnew et al., 2020). Both ¹³Δ and ¹⁸Δ display a typical and distinct range of values for C₃ and C₄ species and depend on environmental factors (Farquhar et al., 1982; Stimler et al., 2011; Adnew et al., 2020). Therefore, the joint COS and

CO₂ measurements allowed investigating the relationship between COS and CO₂ isotope effects, where the CO₂ data provide additional information for validating the experimental setup and the plant behavior.

2. Methods

210

215

220

225

235

2.1. Plant materials and growing conditions

Experiments were conducted with one C₃ plant, sunflower (*Helianthus annuus* "Sunsation"), and an assemblage of stems and leaves from the C₄ plant papyrus (*Cyperus papyrus*). A sunflower in the flowering stage was obtained at a local garden center. A large papyrus shrub was available and grown at the tropical greenhouse at Wageningen Univesity and Research (WUR). Three large stems with leaves were carefully cut from this larger shrub, using a sharp razor, and transported in water to the lab, where they were kept in water throughout the chamber measurements. The sunflower plant and papyrus cuttings were kept under a lamp with a solar-like spectrum (*ca.* 400 μmol m⁻² s⁻¹ PAR, LED growth light SMD2835, Ortho, China) before experiments started and watered sufficiently before and during the measurements. Leaf surface area of sunflower and papyrus were measured after the experiments using a LI-3100 (Li-Cor, Lincoln, NE, USA). This instrument was calibrated using a metal disk with a surface area of exactly 50.00 cm².

230 2.2. Whole plant gas exchange system

Gas exchange experiments were conducted at Wageningen University and Research (WUR) using a custom-built whole plant chamber that was developed for estimating net photosynthetic CO₂ assimilation and transpiration (Lazzarin et al., 2024). The main component is a flow-through plant chamber, which can be fed with different gas mixtures. Two analyzers were used to measure in- and outgoing mole fractions and we used an add-on module for discrete air samples (Fig 2.).

Deleted: T

Deleted: with the

Deleted: A

Deleted: the

Deleted: Sunflower plants

Deleted: were

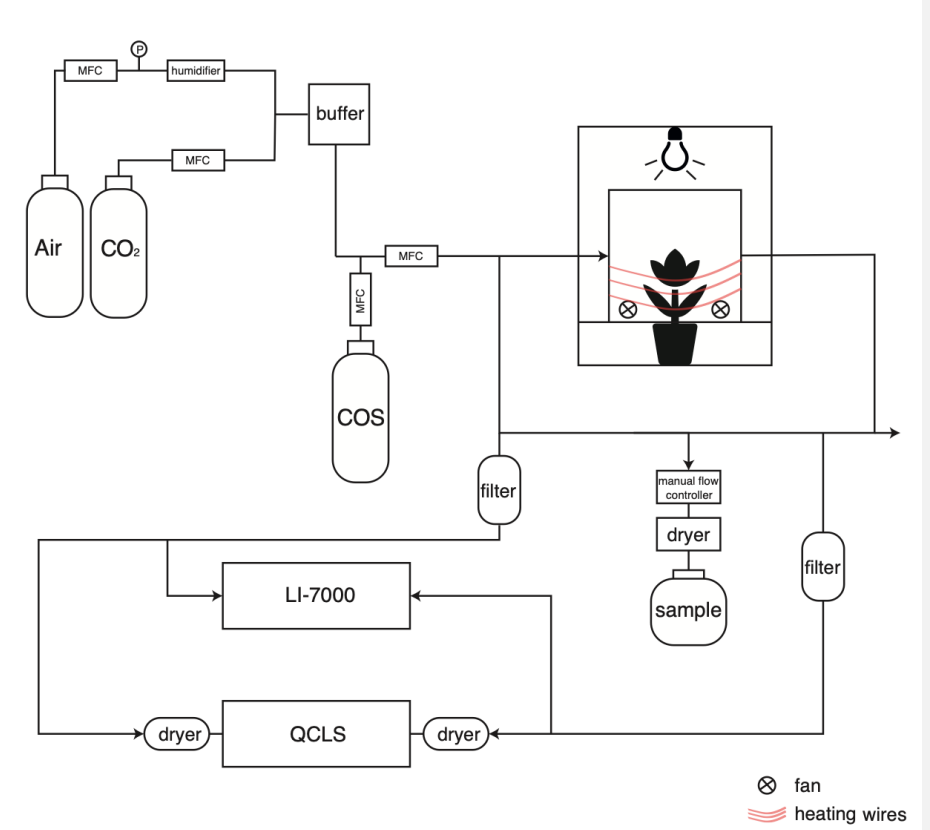
Deleted: In the case of papyrus, t

Deleted: from a larger shrub growing in the tropical greenhouse at Wageningen University and Research (WUR). These leaves w

Deleted: ere

Deleted: with their cut stem

Deleted: and



250 Figure 2. Schematic overview of the setup to determine CO2 and COS photosynthetic isotope discrimination by coupling a custom-built plant chamber to a LI-7000, a QCLS and a system to fill up gas canisters for posterior isotope analysis with IRMS. MFC: mass flow controller; QCLS: Quantum Cascade Laser Spectrometer. CO2 and COS were mixed into humidified synthetic air and introduced into the plant chamber. The in- and outflowing airstreams of the chamber (airin and airoui) were measured by both the LI-7000 and QCLS instruments. Air was dried using Mg(ClO4)2 before the QCLS and when taking a sample for isotope analysis.

The plant chamber was made of clear plexiglass lined with a FEP foil (Holscot Europe, Breda NL) to prevent water from sticking to the chamber walls. The chamber had a diameter of 29 cm, and the height was either 18 or 27 cm, depending on the plant size. To ensure proper air mixing and leaf boundary layer reduction, three SanAce40W ventilators (type 9WL0424P3J001, Sanyo120 Denki, Philippines) were placed in a circular pattern at the bottom of the chamber. Fan speed was controlled with a SanAce PWM controller. The entire chamber was placed inside a 63x63 cm² enclosure with white reflective walls that ensured uniform horizontal light distribution. Air temperature inside the plant chamber was measured with a LM35 temperature sensor (Texas Instruments). Temperature of the plant chamber was controlled using heating cables positioned around the outside of the plant chamber (in combination with a PID controller) and two 12V computer fans were used to provide airflow and cooling around the plant chamber. Light was

260

provided by LED lighting mounted above the chamber with a spectrum resembling sunlight (artificial sunlight research modules generation 2, Specialty Lighting Holland B. V., Breda, the Netherlands). PAR was quantified during the experiments just above the chamber using a handheld PAR sensor (LI-190, Li-Cor, Lincoln, NE, USA). Plants were placed in the chamber, and the bottom two plexiglass panels were closed around the stem of the plant and sealed it with Terostat RB VII, ensuring that the plant was isolated from the soil or water (in the case of the papyrus), and making sure the chamber was leak-free. Two pictures of the plant chamber are shown in Appendix A, Fig. A2.

275

280

285

290

295

300

Synthetic air humidified with a temperature-controlled water bubbler (dew point temperature 17 °C) was mixed with pure CO₂ using mass flow controllers (MFC), to reach the desired CO₂ and H₂O mole fractions. Subsequently, COS from a cylinder with 700 nmol mol⁻¹ COS in synthetic "zero" air was supplied to the mix using a MFC to establish the target COS mole fractions of approximately 2 nmol mol⁻¹. The flow rate of the total (combined) air mixture into the chamber was controlled by a MFC to around 8 L min⁻¹, depending on the experiment conducted. The COS and CO₂ isotopic composition of the ingoing air was determined using the methods described in 2.5 and the values are provided in Table 1.

Table 1. Isotope composition of the inlet gas (air_{in}) supplying the plant chamber determined from samples collected in canisters and analyzed with IRMS. Values are reported on the Vienna Canyon Diablo Troilite (VCDT) (δ^{34} S), the Vienna Pee Dee Belemnite (VPDB) (δ^{13} C) and Vienna Standard Mean Ocean Water (VSMOW) (δ^{18} O) scales.

Plant	δ ³⁴ S COS VCDT (‰)	δ ¹³ C CO ₂ <u>VPDB</u> (‰)	δ ¹⁸ O CO ₂ <u>VSMOW</u> (‰)
Sunflower	11.9 ± 1.2	-23.1 ± 0.1	15.5 ± 0.1
Papyrus	12.1 ± 0.5	-23.0 ± 0.1	15.9 ± 0.1

The CO₂ and H₂O mole fractions of both the in-going air (air_{in}, reference line) and the outgoing air (air_{out}, sample line) of the chamber were analyzed with a LI-7000 infrared gas analyzer (LI-COR Biosciences, Lincoln, Nebraska, USA). To measure the COS mole fractions of air_{in} and air_{out} we used a quantum cascade laser spectrometer (QCLS, TILDAS, Aerodyne Inc, USA) from the Center for Isotope Research, Rijksuniversiteit Groningen (CIO-RUG). This instrument also measured CO₂ mole fractions, which were validated with the readings of the LI-7000 and used for further analyses, QCLS used a 50 mL min⁻¹ flow and was manually switched between air_{in}, air_{out} and calibration cylinders. The air entering the QCLS was dried with magnesium perchlorate (Mg(ClO₄)₂) dryers. Calibration of the QCLS was performed at least twice a day using the working standards from the CIO-RUG, which are calibrated against NOAA-certified cylinders. Possible instrumental baseline drift during the experiments was corrected by measuring pure nitrogen (N₂) multiple times during the experiment. For a detailed description of the QCLS instrument and calibration procedures, see Kooijmans et al. (2017). Blank measurements with an empty chamber were performed before a plant was installed in the chamber to ensure that the COS, CO₂ and H₂O mole fractions of air_{in} and air_{out} were equal.

Samples for isotope analysis of COS and CO₂ were taken in 6 L evacuated Silonite canisters (ENTECH, type: PN: 29-10622) that were then filled to ambient pressure. Sampling was done through a Mg(ClO₄)₂ dryer and a filter, and the flow into the canisters was regulated using a manual flow controller. The dryer was changed after every two samples. At the start of each experiment, two canister samples were collected from air_m, and their average mole fraction and isotope values (Table 1) were used to characterize the incoming air. At each new light setting, and after photosynthetic gas exchange was stable (as monitored with the QCLS and with the LI-7000), two samples were taken

Deleted: ppb

Deleted: ppb

Deleted: CO2 and COS mole fractions of the

Deleted: (reference)

Deleted:

Deleted: (sample) lines were also measured with a

Deleted: The

from air_{out} . For PAR ≥ 0 , these two samples were treated as duplicates and their average mole fraction and isotope values were used for subsequent analyses. In the dark, the plant was still gradually adjusting over time (e.g. closing its stomata) and therefore, these two air_{out} samples were not treated as duplicates and their individual data points are reported.

2.3. Experimental conditions

310

315

320

325

330

335

340

For all experiments, the chamber was supplied with air mixtures with [COS] = 2300–2400 pmol mol $\frac{1}{2}$ and [CO2] = 430–440 µmol mol $\frac{1}{2}$ at a flow rate of 8.1 L min $\frac{1}{2}$, giving an air residence time of around 1.5–2 min. Temperature in the chamber was 24.6–25.0 °C in sunflower experiments and 25.7–25.9 °C in papyrus experiments, chosen to obtain sufficient COS uptake flux (for isotope analysis) while avoiding condensation of water vapor in the system. Light intensity was sequentially set to PAR = 400, 600, 200, and 0 µmol m $^{-2}$ s $^{-1}$, allowing time after each light setting for plant adjustment, uptake flux stabilization and subsequent isotope sampling. Measurements at PAR 600 µmol m $^{-2}$ s $^{-1}$ were not performed with the papyrus due to time constrains. For the dark measurements, chamber light was switched off and the chamber was covered with a blanket.

2.4. Uptake flux calculations

Both CO₂ and COS net uptake fluxes (A^s in pmol m⁻²s⁻¹ and A^c in µmol m⁻²s⁻¹) were calculated using Eq. (5) (which shows the calculation for COS):

$$A^{s} = \frac{u_{e}}{S} \left(C_{e}^{s} - C_{a}^{s} \frac{1 - w_{e}}{1 - w_{a}} \right), \tag{5}$$

where u_e is the molar flow of air entering the chamber (mol air s^{-1}), S is the leaf area (m²), and w_e and w_a (mol of H₂O mol air⁻¹) are the mole fractions of water vapor in air_{in} and air_{out}, C_e^s and C_a^s (pmol COS mol air⁻¹) are the [COS] in air_{in} and air_{out}, respectively.

The uncertainties of the uptake fluxes were calculated by propagating the uncertainties of the in- and outgoing air mole fraction measurements. In the case of the mole fraction measurements by the QCLS, the 1σ uncertainties were obtained measuring air or air out during 15 minutes.

As a consistency check, we also calculated the uptake fluxes using the CO₂ and COS mole fractions determined with the mass spectrometer in the canister samples. Comparison of fluxes determined by both methods lead to the exclusion of two samples because of suspected contamination (see Fig. A1 in Appendix A). QCLS COS and CO₂ fluxes, excluding these two samples, were used in subsequent analyses.

From the CO₂ fluxes, the water vapor fluxes obtained from the LI-7000 analyzer and the leaf temperature, we calculated C_i^c/C_a^c using the gas exchange calculations by Farquhar et al. (1980) (details in Appendix B). The leaf internal COS mole fraction, C_i^S , was calculated using Eqs. (6) and (7), including a ternary correction:

$$C_i^s = \frac{\left(g_t^s - \frac{E}{2}\right)C_a^s - A^s}{g_t^s + \frac{E}{2}},\tag{6}$$

where g_t^s is the total leaf conductance to COS from ambient air to the internal leaf space (C_i^s) (Eq. (7)).

Deleted: Sampling for COS and CO₂ isotope composition started after ingoing and outgoing concentrations had stabilized, to ensure stable rates of photosynthesis, respiration, and COS assimilation. The stability of these fluxes, prior to sampling, was assured by checking the online data of the QCLS and LI-7000.

Deleted: ppt

Deleted: ppm

Deleted: At the start of each experiment with a new plant, two samples were taken of the in-going air (air_{in}). Samples were collected in 6 L canisters from air_{in} (at the start of each experiment with a new plant) and air_{out} (at each light setting).

Deleted: from measurements during which either air_{in} or air_{out} was being measured, which was usually around 15 minutes....

$$g_t^s = \frac{1}{\frac{1.94}{g_b^w} + \frac{1.56}{g_b^w}} \tag{7}$$

Here, g_b^w is the boundary layer conductance to water, which was assumed infinite, as the chamber fans created well-mixed air. The coefficients 1.94 and 1.56 (mol H_2O mol COS^{-1}) are the ratios of diffusivities of COS to water vapor in air and in the boundary layer, respectively (Fuller et al., 1966; Farquhar & Lloyd, 1993). Equations (6) and (7) assume that the leaf internal spaces are saturated with water vapor. This assumption has been questioned, particularly under high avaporative demands (Cernusak et al., 2018; Cernusak et al., 2024), which were not the conditions during our experiments. Further details on gas exchange calculations are presented in Appendix B_{\bullet}

From the CO³⁴S isotope discrimination values ($^{34}\Delta$, Eq. (4)), we estimated the COS mole fraction in the mesophyll cell (C_m^S), using Eq. (8).

$$C_m^s \cong \frac{C_a^s(\Delta^{34}S - a_b) + C_s^s(a_b - a_s) + C_i^s(a_s - a_m)}{\sqrt{1 - a_m}},$$
(8)

where the diffusion fractionation components of a were split into fractionation occurring during boundary layer diffusion ($a_b = 3.5$ %), stomatal diffusion ($a_s = 5.2$ %) and mesophyll diffusion ($a_m = 0.5$ %). C_s^s is the COS mole fraction at the leaf surface, calculated using Eq. (B14), assuming infinite g_b^w , and h (=15 %) is the fractionation occurring during COS hydrolysis by CA (Eq. (4)). The values for all these fractionation factors are from Davidson et al (2022).

Using a big leaf approach, we applied Eqs. (6) to (8) to entire plants excluding roots (sunflower) or several leaves (papyrus). This approach assumes that the entire canopy behaves as a single unshaded leaf. In reality, gradients in light or temperature occur within the canopy, but those should have been minor in our experiment that used small plants in a well-mixed chamber. Additionally, given the precision at which the COS isotope exchange can currently be determined, we deemed it unnecessary to go beyond the big leaf approach.

2.5. Isotope ratio measurements

360

365

370

375

380

385

390

COS and CO2 isotope ratios in the canister samples were determined using isotope ratio mass spectrometry (IRMS) at Utrecht University. Before measurement, the sample canisters' pressure was increased by adding COS-free zero air, as the extraction system needs overpressure. The δ^{34} S in COS was determined according to the methods described in Baartman et al. (2022) but using a new Delta V Plus mass spectrometer, which was specifically customized to measure COS isotope ratios with improved performance (Thermo Fisher Scientific, USA). The continuous-flow GC-IRMS system measures the S⁺ fragment ions generated in the IRMS ion source by the electron-impact fragmentation of COS. The isotope ratios were calculated relative to our laboratory standard, which is a 50 L cylinder, filled with outside air and spiked with COS to approximately 800 pmol mol⁻¹ COS. This lab standard was calibrated against the Vienna Canyon Diablo Troilite (VCDT) international sulfur isotope standard (see Baartman et al., 2022 for a detailed description of the COS isotope measurement system). The typical reproducibility error for δ^{34} S in COS was 0.4 % and the typical uncertainty for a single sample measurement with ambient COS mole fraction was 0.9 % (Baartman et al., 2022).

Deleted: ventilators

Deleted: a

Deleted: chambe

Deleted: Equations 6 and 7 assume that the leaf internal spaces are saturated with water vapor. This assumption has been questioned, particularly under high avaporative demands (Cernusak et al., 2018; Cernusak et al., 2024), which were not the conditions during our experiments. Further details on gas exchange calculations are presented in Appendix B.

Deleted: c Deleted: cDeleted: SDeleted: c Deleted: c Deleted: again Deleted: estimated Deleted: s Deleted: Deleted: Formatted: Font: 10 pt Formatted: Font: 10 pt

Deleted: Further details and the derivations of these calculations can be found supplementary material S3.

Formatted: Normal, Indent: First line: 1.27 cm, No bullets

Deleted:

Deleted: therefore had

Deleted: ppt

Deleted: iol

or numbering

Deleted: 1

Deleted: and

The $\delta^{13}C$ and $\delta^{18}O$ in CO_2 were measured using a separate continuous flow IRMS system, initially developed for measuring CO isotopologues (Pathirana et al. 2015), and later modified to measure CO_2 isotopologues. A laboratory reference air cylinder with known isotopic composition was used for calibration (Brenninkmeijer, 1993). Typical precision was better than 0.2% for both $\delta^{13}C$ and $\delta^{18}O$. Values are reported on the Vienna Pee Dee Belemnite (VPDB) ($\delta^{13}C$) and Vienna Standard Mean Ocean Water (VSMOW) ($\delta^{18}O$) scales.

2.6. Isotope discrimination calculations

425

435

440

445

450

455

Observed isotope discrimination (‰) was calculated using Eqs. (9) and (10) (Evans et al. 1986):

$$\Delta = \frac{\xi(\delta_a - \delta_e)}{1000 + \delta_a - \xi(\delta_e - \delta_a)},\tag{9}$$

where δ_e and δ_a are the isotope compositions of the gas entering and leaving the chamber, respectively, for the gas of interest (δ^{13} C, δ^{18} O in CO₂, or δ^{34} S in COS). ξ is calculated as:

$$\xi = \frac{C_e}{C_e - C_a},\tag{10}$$

where C_{eq} and C_{eq} are the mole fractions (CO₂ or COS), entering and leaving the chamber, respectively. The errors on the measured mole fractions and isotope ratios were propagated to the isotope discrimination values (Δ); details are provided in the supplementary material.

3. Results and Discussion

3.1. COS and CO₂ uptake fluxes

In experiments with both plant species there was a net uptake of COS under all light conditions, including dark (Fig. 3b). Mean COS uptake fluxes in the light were 73.3 ± 1.5 pmol m⁻² s⁻¹ and 107.3 ± 1.5 pmol m⁻² s⁻¹ for sunflower and papyrus, respectively, and uptake fluxes did not vary strongly for different light conditions. Note that samples in the dark were taken sequentially, when plant performace was still adjusting.

Previously reported COS uptake fluxes at the cosystem scale usually range between 30 and 60 pmol m⁻² s⁻⁴ (Cho et al., 2023; Kooijmans et al., 2017; Commane et al., 2015; Billesbach et al., 2014), with some higher reported uptake fluxes around 80 to 100 pmol m⁻² s⁻¹ (Asaf et al., 2013; Spielmann et al., 2023). Berkelhammer et al. (2020) reported maximum mid-day ecosystem-scale COS uptake fluxes of up to 100 pmol m⁻² s⁻¹ for a maize field (C₄) during July. Those values were higher than the mid-day fluxes obtained from a prairie (C₃ and C₄ species), being around 50 pmol m⁻² s⁻¹ (July – August). However, Stimler et al. (2011) measured COS fluxes of only around 30 pmol m⁻² s⁻¹ under similar light intensity, in leaf cuvette experiments. Thus, our measured COS uptake fluxes are at the high end of the spectrum.

Stomatal conductance to water vapor in sunflower ranged from 0.25 to 0.35 mol m⁻² s⁻¹ under light conditions and decreased to 0.15 mol m⁻² s⁻¹ in the dark (Table 2). In papyrus, stomatal conductance was slightly higher in the light, ranging between 0.27 and 0.39 mol m⁻² s⁻¹. In the dark, stomatal conductance for papyrus dropped substantially to 0.09 mol m⁻² s⁻¹ during the first sampling and further to 0.04 mol m⁻² s⁻¹ during the second. This is reflected in the lower COS assimilation for papyrus in the dark compared to sunflower (see Fig. 3 and Table 2).

Deleted: The COS and CO_2 isotopic compositions of the gas entering the chamber are given in Table 1.

Deleted: c_{in}

Deleted: Cout

Deleted: of the gas of interest

Deleted: in our case

Deleted: At the start of each experiment, two canister samples were collected from the chamber inlet and their average was used to characterize $air_{\rm in}$ ($c_{\rm in}$ and $\delta_{\rm in}$, Table 1), which was assumed constant over the experiment as it was supplied from a cylinder.

Deleted:

Deleted: Table 2. Isotope composition of the inlet gas (air_{in}) supplying the plant chamber determined from samples collected in canisters and analyzed with IRMS.

Plant

Formatted

Deleted: 4

Deleted: 2

Deleted: 9

Deleted: 2

Deleted: 5.5

Deleted: conditions

Deleted: condition

Deleted: ere

Deleted: Therefore, these samples were not treated as duplicates. As hydrolysis of COS, catalyzed by CA, is a light-independent reaction, COS assimilation can continue as long as the stomata are open (Protoschill-Krebs et al., 1996).

Deleted: canopy- or

Formatted: Indent: First line: 1.27 cm

Deleted:, which may be due to the high ambient COS mole fraction inside the chamber

495

500

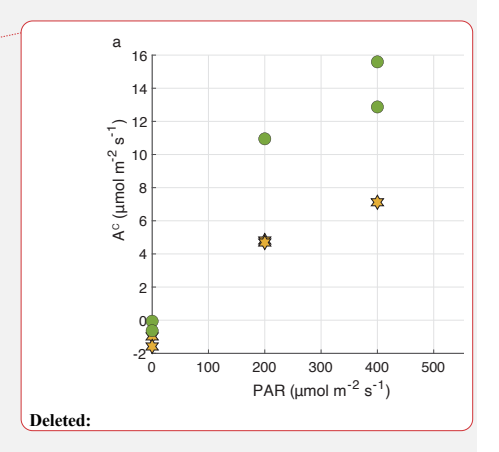
Overall, our observed stomatal conductance values are at the upper end of the previously reported ranges. For example, Stimler et al. (2011) reported g_s values of up to approximately 0.17 mol m⁻² s⁻¹, while Berkelhammer (2020) found maximum g_s values of around 0.22 mol m⁻² s⁻¹ for maize (C₄) and 0.12 for a prairie field (C₃ and C₄). Miner & Bauerle (2017) did find unusually high stomatal conductance values for sunflowers of up to 1.2, with a high inter-plant variability and Howard & Donovan (2007) reported nighttime g_s values of 0.023-0.225 for well-watered sunflowers. These elevated g_s values in our experiments likely explain the relatively high and stable COS fluxes for PAR > 0. Moreover, the non-zero g_s values under PAR = 0 support the continued COS uptake in the dark, particularly for sunflower (Figure 3b). As hydrolysis of COS, catalyzed by CA, is a light-independent reaction, COS assimilation can continue as long as the stomata are open (Protoschill-Krebs et al., 1996).

The small increase in C_i^S/C_a^S values (Table 2) with increasing PAR also suggests that stomata were sufficiently open to sustain stable COS uptake fluxes, even in low-light conditions. In plant experiments conducted with elevated COS mole fractions (1.5 nmol mol⁻¹), Stimler et al. (2010) reported similar C_i^S/C_a^S values around 0.6, corresponding to COS uptake fluxes around 100 pmol m⁻² s⁻¹ and g_s of 0.5 mol m⁻² s⁻¹. Thus, the higher than usual C_i^S/C_a^S and potentially the higher stomatal conducance in our experiments may be attributable to the elevated COS mole fractions in our chamber. These elevated COS mole fractions were necessary for obtaining precise measurements of COS isotope discrimination.

Formatted: Indent: First line: 1.27 cm

Formatted: Superscript

Formatted: Indent: First line: 1.27 cm, Line spacing: 1.5



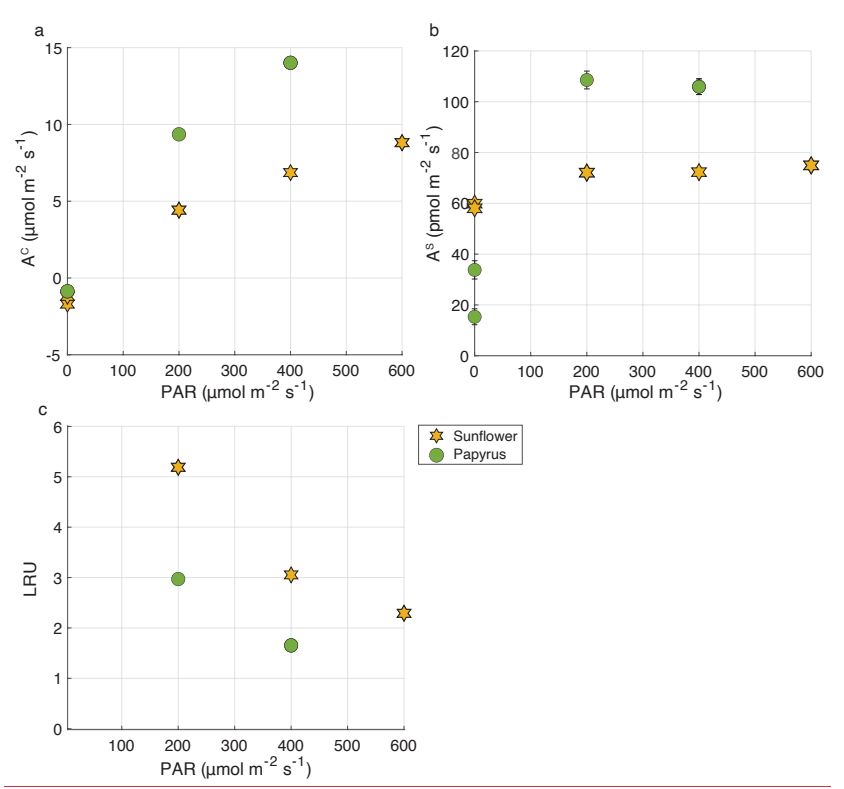


Figure 3. a. A^{C} (CO2 uptake flux, in μ mol m^{-2} s⁻¹). b. A^{S} (COS uptake flux, in μ mol m^{-2} s⁻¹) and c. μ RU versus μ AR (μ mol μ -2 s⁻¹), for sunflower (orange stars) and papyrus (green circles). Flux values for μ AR > 0 are means μ 1 standard error (SE) (μ 1 = 2), where 1 SE was obtained using error propagation (see supplementary materials), flux values for μ AR = 0 reflect individual measurements. Only positive LRU values are shown. LRU was negative for μ AR = 0 (see Table 2). Errors are only displayed when larger than the symbols.

515

520

Both sunflower and papyrus respired CO₂ in the dark and photosynthesyzed in the light, at a net rate that increased with PAR (Fig. 3a). Mean CO₂ uptake fluxes in light conditions were $6.7 \pm 1.7 \,\mu\text{mol m}^{-2} \,\text{s}^{-1}$ for sunflower and $11.7 \pm 2.2 \,\mu\text{mol m}^{-2} \,\text{s}^{-1}$ for papyrus (Fig. 3a). These photosynthesis rates match that of sunflowers of Tezera et al. (2008) under their low-light condition experiments (in the least drought-exposed conditions).

At all light intensities (PAR \geq 0), CO₂ uptake rates were larger in papyrus than in sunflower, matching expectations for C₄ vs. C₃ photosynthesis (Farquhar & Lloyd, 1993). Our measurements can be classified as relatively low-light, because although the PAR measured at the top of the chamber was 400 µmol m $^{-2}$ s $^{-1}$ at the highest setting for the C₄ experiments, there was likely light attenuation across the plant canopy. The photosynthesis rates for papyrus are comparable with previous measurements, conducted under low-light conditions. Ubierna et al., (2013) measured CO₂ assimilation rates of around 10 µmol m $^{-2}$ s $^{-1}$ at PAR \equiv 500 µmol m $^{-2}$ s $^{-1}$ in three C₄ species, *Zea mays*, *Miscanthus*

Deleted: panel a,

Deleted: and

Deleted: panel b,

Deleted: (

Deleted: ,

Deleted: For CO2, both

Deleted: performe

Deleted: d

Deleted: respiration

Deleted: is

Deleted: The photosynthesis rates for papyrus are comparable with previous measurements, conducted under low-light conditions.

Deleted: reached

Deleted: PAR that was received by the plant leaves was likely lower, especially considering that some leaves were (partially) shaded or received diffused light, reflected off the outer enclosure walls.

Deleted: also found

Deleted: for

Deleted: levels of

x giganteus and Flaveria bidentis, under varying light conditions between 0 and 2000 μ mol m⁻² s⁻¹. Their results are similar to our measured CO₂ uptake fluxes of between 9.4 μ mol m⁻² s⁻¹ (200 PAR) and 14.0 μ mol m⁻² s⁻¹ (400 PAR).

545

550

555

560

565

570

At PAR = 600 μmol m⁻² s⁻¹, LRU (Eq. (1)) was 2.3 ± 0.08 for sunflower and at PAR = 400 μmol m⁻² s⁻¹, LRU values were 3.A₄ ± 0.11 and 1.A₅ ± 0.06 for sunflower and papyrus, respectively (see Table 2 and Fig. 3). As PAR decreased to 200 μmol m⁻² s⁻¹, LRU increased to 5.2 ± 0.16 for sunflower and 3.0 ± 0.11 for papyrus. The increase in LRU at low light was due to a decrease in CO₂ uptake fluxes while the COS uptake remained roughly constant. In the dark, LRU values were negative, up to −16.0 for sunflower, as COS uptake by the plant continued while CO₂ was being respired. Our LRU values are higher than those found by Stimler et al. (2011) and higher than the usually reported median LRU values of 1.7 (n = 53) for C₃ species and 1.2 (n = 4) for C₄ (Whelan et al., 2018), which may be due to our relatively low-light experiments. Still, previously reported LRU values display a wide range of values of between 0.7 and 6.2, and Stimler et al. (2011) also reported a higher LRU for C₄ compared to C₃. Furthermore, recent research has shown that LRU can differ across species and vary with environmental conditions, especially light availability and VPD (Kooijmans et al., 2019; Spielmann et al., 2023; Sun et al., 2022). The exact mechanism for this varying LRU is still not completely understood (Whelan et al., 2018; Wohlfahrt et al., 2023).

Our slightly high LRU values could also be due to the higher than ambient COS mole fractions (of around 2 nmol mol⁻¹) that the plants were exposed to during our experiments. Davidson et al. (2022) reported LRU values or 0.7 and 1.7 for C₃ and C₄, respectively for experiment with ambient COS mole fractions, and LRU values of 2.4 and 1.0 for C₃ and C₄ for plants exposed to 2900 nmol mol⁻¹ CO₂ and 3.4 nmol mol⁻¹ COS (see Appendix C). Thus, exposure to higher COS mole fractions could have influenced LRU, however, in the experiments by Davidson et al (2022), not only the COS but also the elevated CO₂ mole fractions could have affected the LRU (Sun et al., 2022).

Figure 4 shows the CO₂ uptake flux (µmol m⁻² s⁻¹) plotted against ratio of the CO₂ mole fractions in the intercellular space versus the ambient (Table 2) (C_i^C/C_a^C) . The C_i^C/C_a^C ratio increases with decreasing CO₂ uptake flux for both species and the differences in CO₂ uptake flux between C₃ and C₄ are consistent with the results presented by Stimler et al. (2011). Our measured C_i^C/C_a^C for sunflower compares well with previous values for sunflower of 0.8 found by Tezara et al. (2008). The C_i^C/C_a^C for papyrus is high for a C₄ species, for which values usually range around 0.4, but could again be explained by the low-light conditions, as previously observed by Ubierna et al., (2013). The higher than usual C_i^C/C_a^C could also be explained by the fact that we measured entire plants, of which some leaves were partly shaded.

Deleted:

Deleted:

Deleted: 0

Deleted: 6

Deleted:

Deleted:

Deleted: Yet

Deleted: vary

Deleted: 2ppb

Deleted: ppm

Deleted: ppb

Deleted: more research is needed to quantify this effect

Deleted: Furthermore, recent research has shown that LRU can differ across species and vary with environmental conditions, especially light availability and VPD (Kooijmans et al., 2019; Spielmann et al., 2023). The exact mechanism for this varying LRU is still not completely understood (Whelan et al., 2018; Wohlfahrt et al., 2023).

Deleted: versus

Deleted:

Deleted: ratio,

Deleted: which

Deleted: . The species

Deleted: c_i/c_a

Deleted: generally

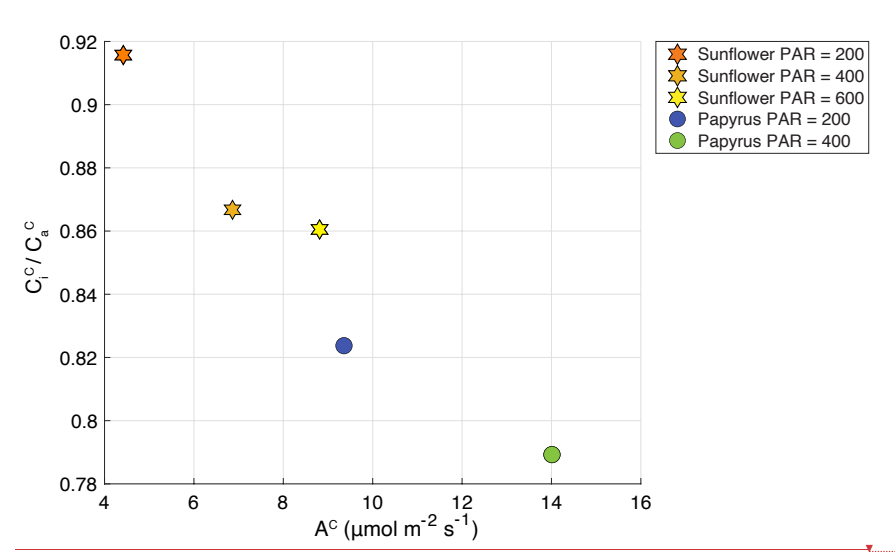


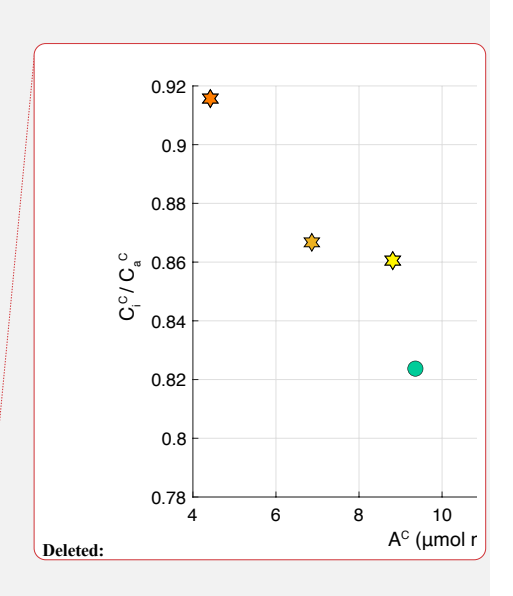
Figure 4. C_c^C/C_a^C plotted against A^C (CO₂ uptake flux in μ mol m^{-2} s⁻¹), for sunflower (stars) and papyrus (circles). Colors indicate PAR levels (μ mol m^{-2} s⁻¹). Data for PAR = 0 are not included because the plants were respiring during dark conditions.

3.2 CO34S discrimination

600

605

Table 2 shows the isotopic discrimination for COS $\binom{34}{6}\Delta$) and CO₂ $(^{13}\Delta, ^{18}\Delta)$, and accompanying data for the different light treatments. In contrast to the CO₂ isotope discrimination (Sect. 3.3), $^{34}\Delta$ did not show a trend with COS uptake flux nor with PAR (Fig. 5), C_L^S/C_a^S (Fig. 6), or a difference between the species. The average $^{34}\Delta$ values in light conditions (PAR > 0) were 3.4 ± 1.0 (SEM) % for sunflower and 2.6 ± 1.0 (SEM) % for papyrus (see Table 2). For sunflower in dark conditions, we found a $^{34}\Delta$ of 4.7 ± 1.5 % for the first sample and 1.3 ± 1.6 % for the second sample. The COS uptake flux for papyrus in dark conditions decreased drastically, to the point that $^{34}\Delta$ could no longer be estimated with confidence (see Fig. 3).



Formatted: Font: Not Bold

Deleted: and

Deleted: 0.8

Deleted: 0.3

Deleted: , giving an average $^{34}\Delta$ of 3.0 ± 2.3 ‰

Table 2. Photosynthetic discrimination (mean ± 1 SE, n = 2), COS and CO₂ uptake fluxes (A^S and A^C), LRU, stomatal conducance to water vapor (g_{SW}), total conductance to COS (g_t^S) , leaf internal vs. ambient mole fraction ratios for COS (C_i^S/C_a^S) and CO₂ (C_i^C/C_a^C) , mesophyll vs. ambient COS mole fraction (C_m^S/C_a^S) for sunflower and papyrus, for each PAR level. The uncertainties were calculated as the standard error of the mean (SEM) and the student's t-distribution, with 60% confidence interval and 1 (=n-1) degree of freedom. <u>Uncertainties where n = 1 are the propagated measurement uncertainties.</u> Values without stated uncertainty are single sample measurements (in the case of isotope discrimination values) or have an uncertainty smaller than 0.01 (in the case of $C_a^{\Gamma}/C_a^{\Gamma}$ and C_m^s/C_a^s). As at PAR = 0 for papyrus was too small for calculating $^{34}\Delta$. The samples taken in the dark were not seen as duplicates as the plant was still adjusting to the dark conditions between sampling, and two values for PAR = 0 are given for each species.

Plant	PAR (µmol	Number of	³⁴ ∆ (‰)	¹³ ∆ (‰)	¹⁸ ∆ (‰)	A ^S (pmol	A ^C (<u>u</u> mol	LRU	g_{sw} (mol	g_t^s (mol	g_t^c (mol	C_i^S/C_a^S	C_m^S/C_a^S	$C_i^{\mathcal{C}}/C_a^{\mathcal{C}}$	
	$m^{-2} s^{-1}$)	samples				m ⁻² s ⁻¹)	m ⁻² s ⁻¹)		<u>m⁻² s⁻¹)</u>	m ⁻² s ⁻¹)	m ⁻² s ⁻¹)				7
Sunflower	200	<u>2</u>	3.6 ±	32.4	148.7 ±	72.1_±	4.42 <u>±</u>	5.2 ± 0.16	0.25	0.13	<u>0.16</u>	0.50	0.11	0.91	
			1.6	± 1.1	0.7	1.9	0.02						$(n = 1)^{c}$		
Sunflower	400	1	3.7_±	24.9	83.6±	72.3 ±	6.86 <u>±</u>	3.1 ± 0.11	0.26	0.14	0.16	0.52	0.07	0.86	1
			2.3	± 1.5	1.5	2.2	0.02								
Sunflower	600	<u>2</u>	2.8 ±	23.6	63.8 ±	74.9 <u>±</u>	8.81 <u>±</u>	2.3 ± 0.08	0.35	0.18	0.22	0.62	0.04	0.87	
			1.7	± 1.2	0.9	<u>2.1</u>	0.02								
Sunflower ^a	0	1	4.7 ±	-	-	5 9.9 ±	-	-	0.16	0.08	<u>0.10</u>	0.45	-	_	
			1.5			1.9									1
Sunflower ^a	<u>0</u>	1	1.3 ±	_	_	58.0 ±	_	_	0.15	0.08	0.09	0.45	_	_	
			1.3			1.8									1
Papyrus	200	1	2.5 ±	21.8	79.4 ±	108.6 ±	9.36 ±	3.0 ± 0.11	0.27	0.14	0.17	0.39	0.05	0.82	
			1.6	± 1.5	1.5	3.5	0.04								
Papyrus	400	2	2.6 ±	18.9	49.4 ±	105.9 <u>±</u>	14.01 <u>±</u>	1.7 ± 0.06	0.39	0.20	0.24	0.58	0.03	0.79	
			<u>1</u> ,4	± 3.4	0.4	3.1	0.08						$(n = 1)^{c}$		
Papyrus ^b	0	1	-	-	-	33.8 ±	-	-	0.09	0.05	0.05	0.60	_		
						3.6									1
Papyrus ^b	<u>0</u>	1	Ξ	Ξ	=	$\frac{15.3 \pm}{3.1}$	Ξ	Ξ	0.04	0.02	0.03	0.66	Ξ		,

^aThere was no uptake of CO_2 at PAR = 0

Deleted: ¶	([2]
Deleted:	
Deleted:	
Deleted:	
Formatted	([3]
Deleted: deviation	
Formatted	([4]
Deleted: As,	
Deleted: μ	
Deleted: p	
Formatted	([5]
Formatted	([7]
Deleted: 2	
Formatted	([6]
Deleted: 0.6	
Deleted: a	
Deleted: 3.0 ± 2.3	
Deleted: 59.0 ± 1.31	
Formatted	([8]
Formatted	([10]
Deleted: 0	•
Formatted	([9]
Deleted: 24.6 ± 13.1	
Deleted: 0.72 ± 0.16	
Formatted	([11]
Formatted	([12]
Formatted	([13]
Formatted	([15]
Formatted	([14]
Formatted	([16]
Formatted	([17]

bThere was no uptake of CO_2 at PAR = 0 and not sufficient COS uptake to calculate $^{34}\Delta$

 $[\]mathcal{L}_{m}^{S}$ / \mathcal{L}_{m}^{S} only obtained from one sample as the calulations for the other sample yielded negative (unrealistic) values for \mathcal{L}_{m}^{S}

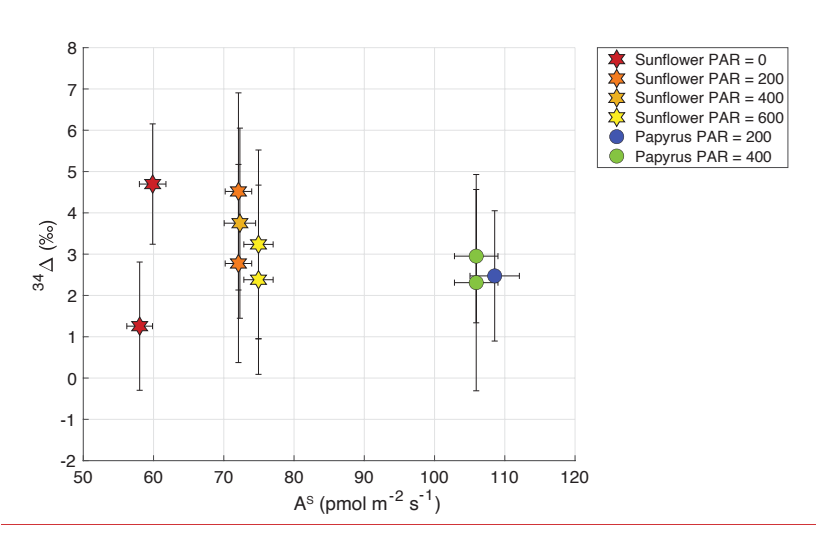


Figure 5. Plant COS isotope discrimination ($^{34}\Delta$) plotted against A^S (COS uptake flux in pmol m^{-2} s $^{-1}$) for sunflower (stars) and papyrus (circles). Colors indicate PAR levels (until m^{-2} s $^{-1}$). Samples for PAR = 0 are only shown for sunflower as A^S for papyrus (PAR = 0) was too low to calculate $^{34}\Delta$ with meaningful precision.

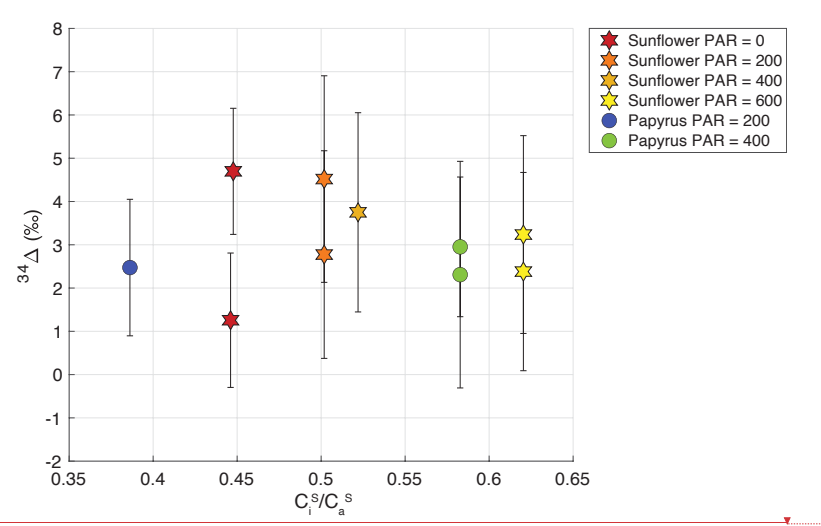
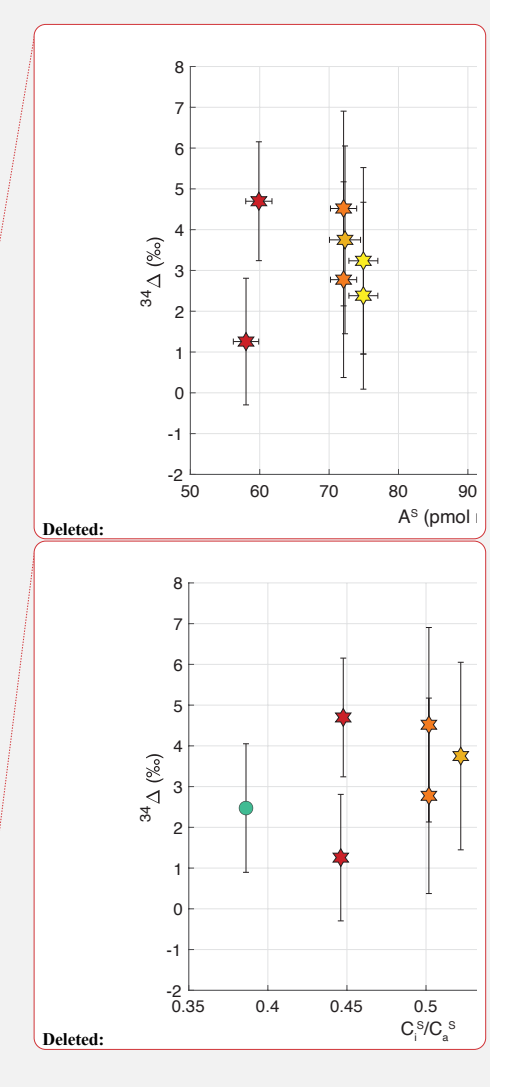


Figure 6. Plant COS isotope discrimination ($^{34}\Delta$) against the ratio of internal versus C_i^S/C_a^S , for sunflower (stars) and papyrus (circles). Colors indicate PAR levels (µmol m^{-2} s⁻¹). Samples for PAR = 0 are only shown for sunflower as A^s for papyrus (PAR = 0) was too low to calculate $^{34}\Delta$ with meaningful precision.





To further investigate this lack of variability in $^{34}\Delta$, we examined the variability in C_i^S/C_a^S and C_m^S/C_a^S as a function of PAR (Table 2). We observed a slight increase of C_i^S/C_a^S with PAR that could be explained by an increase in g_8 with available light. Observed COS isotope discrimination also depends on C_m^S/C_a^S , the ratio of COS mole fractions in the mesophyll cell and the ambient air (see Eq. (4)). This ratio was relatively stable at low values around 0.03 \pm 0.07 (Table 2), over the various PAR levels and did not differ substantially between sunflower and papyrus, except for one sunflower sample (PAR = 200) yielding a $C_m^S/C_a^S = 0.11$. This lack in variability in $C_m^S/C_a^S = 0.11$ in the absence in variability in $C_m^S/C_a^S = 0.11$ in the absence in variability in $C_m^S/C_a^S = 0.11$ in Appendix B), and thus, the results should not be over interpreted.

Comparing our ³⁴ Δ to previous studies. Angert et al. (2019) estimated a value for ³⁴ Δ during COS plant uptake of around 5 ‰ (based on binary diffusion theory), and experiments presented by Davidson et al. (2021) and Davidson et al. (2022) yielded ³⁴ Δ values of 1.6 ± 0.1 ‰ for C₃ and 5.4 ± 0.5 ‰ for C₄ species. Our results differ from these measurements, as we did not find statistically different ³⁴ Δ values between our C₃ and C₄ species. However, the range for ³⁴ Δ that we measured in sunflower of 2.8 ± 1.7 ‰ to 3.7 ± 2.3 ‰ (average 3.3 ± 1.0 (SEM) ‰) is in the same range as the C_{3.7} ³⁴ Δ found by Davidson et al. (2021; 2022) and the theoretical estimate of Angert et al. (2019). This is reassuring, given that different measurement techniques were used for both the plant experiments (flow-through chamber compared to closed-chamber) and the isotope ratio measurements.

The benefit of using a flow-through system is that stable environmental conditions inside the chamber can be maintained during the experiment. In contrast, in a closed chamber, CO₂ and COS mole fractions will decrease due to plant uptake, which can be problematic when the experiment runs over long periods of time. Furthermore, transpiration by the plant will increase the water vapor mole fraction in the chamber, which might affect stomatal opening and therefore also the isotope fractionation.

3.3 CO₂ isotope discrimination

675

680

685

690

695

700

705

3.3.1 ¹³CO₂ discrimination

In both sunflower and papyrus, $^{13}\Delta$ increased as the CO₂ uptake flux decreased, with decreasing PAR (Fig. 7). Average $^{13}\Delta$ in sunflower was between 23.6 \pm 1.2 and 32.4 \pm 1.1 % (Table 2), which is within the range of values expected for C₃ photosynthesis (Farquhar et al. 1982, Kohn 2010, Cernusak et al. 2013, Wingate et al., 2007). However, in papyrus, $^{13}\Delta$ was between 18.9 \pm 3.4 and 21.8 \pm 1.5 %; much larger than the expected 3 to 6 % for C₄ species operating at optimal conditions (Farquhar et al 1983; Cerling et al. 1997; Kubásek et al., 2013; Ellsworth and Cousins, 2016; Eggels et al., 2021). As previously explained, our measurements were performed at low light intensities (PAR \leq 400 μ mol m⁻² s⁻¹), which resulted in moderately low photosynthetic rates (9.3-14.0 μ mol m⁻² s⁻¹). In C₄ species, $^{13}\Delta$ has been shown to increase at low light to values as large as 8-17%, when PAR = 50-125 μ mol m⁻²s⁻¹) Cubierna et al. 2013, Pengelly et al. 2010, Kromdijk et al. 2010) and photosynthetic rates were small (<5 μ mol m⁻²s⁻¹) Our $^{13}\Delta$ values for papyrus are still larger than these previous reports at low irradiance, suggesting that processes other than photosynthesis might have affected the measurements. Upward transport of water dissolved CO₂ in the transpiration stream has been shown in tree stems (Aubrey and Teskey, 2009; Bloemen et al. 2013) and in papyrus culms (Li and

Deleted: ,

Deleted: indicating that the stomata were perhaps not at their maximum opening at PAR≤400, which was also suggested by the CO₂ assimilation and isotope discrimination results (Figs. 4 and 7). However,

Deleted: was rather stable at

Deleted: 1

Deleted:

Deleted: 23

Deleted: could

Deleted: .

Deleted: as previous studies (Stimler et al., 2011; Davidson et al., 2021; Davidson et al., 2021; Davidson et al., 2022) attribute the differences in isotope discrimination between C_3 and C_4 species to

Deleted: These are the only studies on COS isotope discrimination during plant uptake that have been conducted to date....

Deleted: nd

Deleted: T

Deleted: that we measured for sunflower

Deleted: n between the

differences in C_m^S/C_a^S .

Deleted: for C₃

Deleted: . However, all $^{34}\Delta$ estimations are roughly in the same range,

Deleted: which

Formatted: Font: Not Bold

Deleted: -

Jones, 1995). We measured detached papyrus leaves submerged in water. This setting could have facilitated the transport of water dissolved CO_2 into the leaf chamber, particularly because papyrus leaves have numerous vascular bundles surrounded by large air cavities (Plowman, 1906). Water dissolved CO_2 would presumably have near-ambient air $\delta^{13}C$ values – enriched compared to tank CO_2 supplied to the chamber air –, and therefore if released in the plant chamber would artefactually increase $\frac{13}{2}\Delta$.

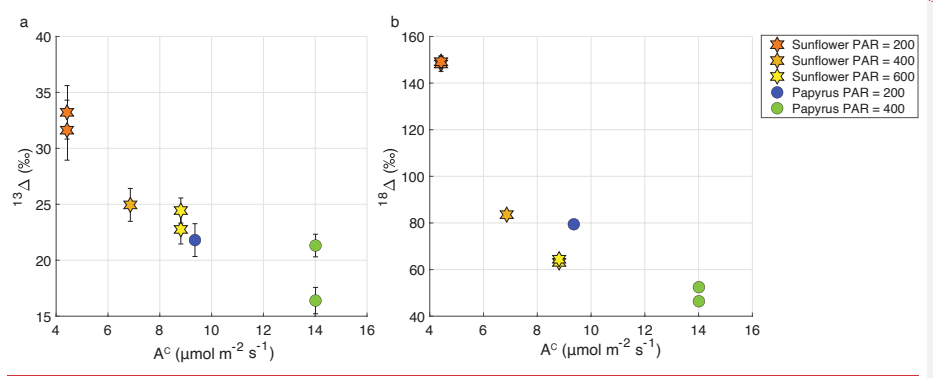


Figure 7. Variation of photosynthetic discrimination against $^{13}\text{CO}_2(^{13}\Delta$, panel a) and $\text{CO}^{18}\Delta$ ($^{18}\Delta$, panel b) as a function of A^C (CO_2 uptake flux in μ mol m^{-2} s⁻¹) for sunflower (stars) and papyrus (circles). Colors indicate PAR levels (μ mol m^{-2} s⁻¹). Data for PAR = 0 are not included because the plants were respiring in during dark conditions.

3.3.2 C¹⁶O¹⁸O discrimination

740

750

755

760

765

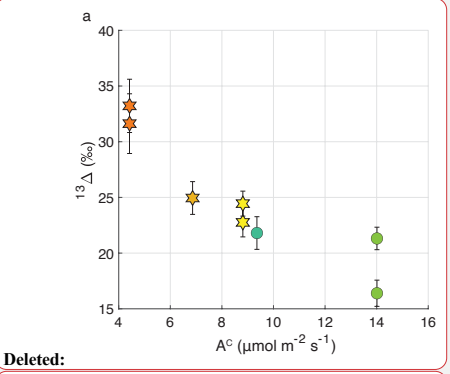
From Fig. 7, we observe a negative relationship between apparent $^{18}\Delta$ and CO₂ uptake flux, similar to $^{13}\Delta$. The average $^{18}\Delta$ values of sunflower range between 63.8 \pm 0.9 and 148.7 \pm 0.7 ‰ and the average $^{18}\Delta$ values of papyrus are between 49.4 \pm 0.4 and 79.4 \pm 1.5 ‰ (Table 2). $^{18}\Delta$ mostly reflects the exchange of 18 O between CO₂ and leaf water (Francey and Tans; Yakir, 1998; Adnew et al., 2020). The lower $^{18}\Delta$ in C₄ species likely indicates the incomplete equilibrium between CO₂ and leaf water, because of the reduced CA activity in C₄ species compared to most C₃ species (Gillon and Yakir, 2000).

A negative correlation of ${}^{18}\Delta$ with CO₂ assimilation and light intensity, as well as lower ${}^{18}\Delta$ in C₄ species was also found by Stimler et al. (2011). For their C₃ plants, they found that ${}^{18}\Delta$ ranged between 40 and 240 %, with the highest values found at the lowest CO₂ uptake fluxes. For C₄ species, Stimler et al. (2011) found an ${}^{18}\Delta$ between 10 and 50 %. Seibt et al. (2006) also found large variations in ${}^{18}\Delta$ during CO₂ uptake by *Picea sitchensis*, and a correlation with PAR. They too measured the largest ${}^{18}\Delta$ discrimination at dusk and dawn, when light intensity was lowest.

The relation between the COS uptake flux and $^{18}\Delta$ can also be analyzed, since both depend on the same diffusion pathway and CA activity (Stimler et al., 2011). Stimler et al. (2011) observed a negative correlation between $^{18}\Delta$ and COS uptake flux, with a larger change in $^{18}\Delta$ for C₃ species, compared to C₄. Figure 8 shows $^{18}\Delta$ against the COS uptake flux for our data. We do not observe such a correlation between $^{18}\Delta$ and the uptake COS flux. However, our range in COS uptake flux for each species is small, as we found that the COS uptake flux did not change

Deleted:

Deleted:



Deleted: Thus, the $^{18}\Delta$ of papyrus is clearly lower than that of sunflower.

Deleted: an

Deleted: which

Deleted: around

Deleted: here

Deleted: were

Deleted: clear

significantly with light intensity. In the same range of COS uptake flux data, Stimler et al. (2011) did not find a strong trend in $^{18}\Delta$ either.

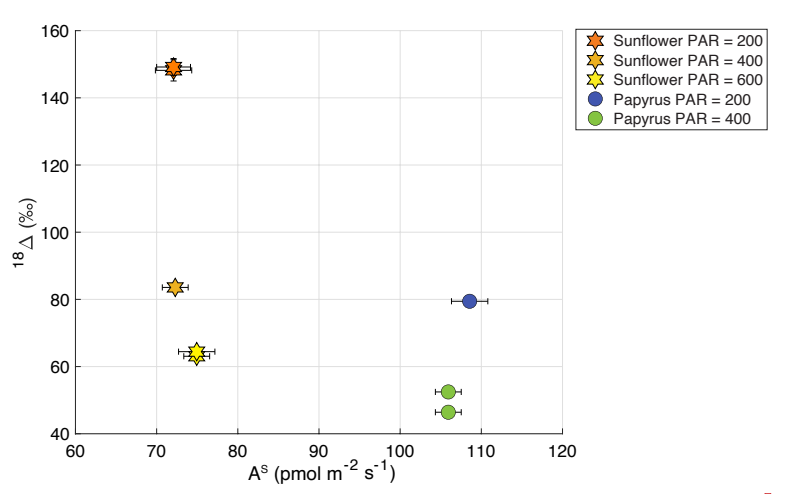


Figure 8. $^{18}\Delta$ (%) plotted against A^S (COS uptake flux in pmol m⁻² s⁻¹) for sunflower (C3) and papyrus (C4), where the different symbols and colors indicate the plant types and PAR (μ mol m⁻² s⁻¹). <u>Data for PAR = 0 are not included because the plants were respiring during dark conditions.</u>

4 Conclusions & perspectives

780

785

790

795

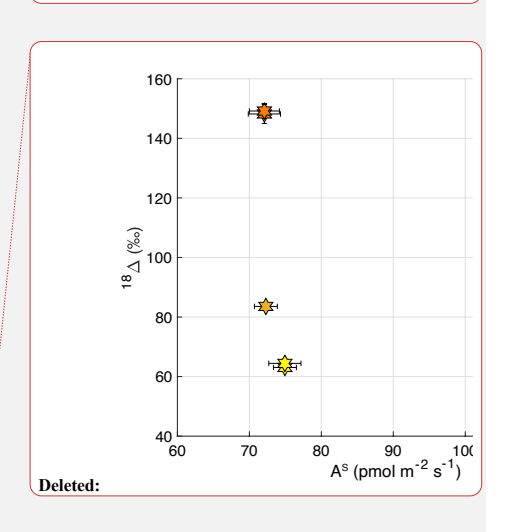
800

This study presented measurements of COS and CO₂ plant uptake fluxes and $\frac{\text{COS}}{4}$ $\frac{2^4\Delta}{4}$ and $\frac{2^4\Delta}{4}$ and

Our study is the first to combine measurements of both COS and CO₂ plant isotope discrimination, where the CO₂ values provided additional information on the plant's behavior and their responses to environmental variation. CO₂ assimilation increased with increasing PAR level and CO₂ uptake flux was higher for the C₄ than for the C₃ species, both findings being consistent with previous results under similar conditions. However, the moderate to low-light conditions were limiting CO₂ assimilation rate. Corresponding CO₂ isotope discrimination values, $^{13}\Delta$ and $^{18}\Delta$, were therefore higher than those normally exhibited by planst at full photosynthetic capacity. $^{13}\Delta$ CO₂ isotope discrimination as well as C_t^C/C_a^C were lower in papyrus than in sunflower, consistent with differences between C₃ and C₄ photosynthesis and C_t^C/C_a^C decreased with light intensity for both species. Therefore, we conclude that both species were behaving normal, albeit not in the most optimal conditions for maximum photosynthetic CO₂ assimilation.

In contrast to photosynthesis, COS assimilation <u>did not vary strongly with light intensity</u>, which is to be expected <u>when stomatal conductance</u> is sufficiently large to maintain a steady COS supply to the mesophyll cell, as

Deleted: when adjusting the



Formatted

Deleted: isotope discrimination factors

Deleted: of COS,

Deleted: of CO₂

Deleted: and

Deleted: reactions

Deleted: changes in

Deleted: conditions

Deleted: ,

Deleted: at maximum capacity for CO2 assimilation rate.

Deleted: as expected

Deleted: capacity for

Deleted: was light-independent,

Deleted: since

the hydrolysis reaction catalyzed by CA is light-independent. The observed COS uptake flux was lower during the dark experiments, but not zero, consistent with residual stomatal opening. Our measurements also showed a constant $^{34}\Delta$ across different light settings, which can be explained by the rather constant C_i^S/C_a^S and C_m^S/C_a^S values. Surprisingly, $^{34}\Delta$ also did not differ significantly between papyrus and sunflower, whereas previous measurements (Davidson et al., 2022) reported higher ^{34}S isotope discrimination for C_4 species. Nevertheless, our values for $^{34}\Delta$ are close to the previously reported values by Davidson et al. (2022), despite using a different experimental set-up and a different way to calculate the isotopic discrimination (Evans et al., 1986).

820

825

830

835

840

845

850

For future studies, we recommend to use representative C₃ and C₄ plant species to characterize isotope discrimination more broadly. In our study, papyrus was selected due to its availability and large leaf area, which enabled sufficient COS uptake fluxes for isotope analysis at the required precision. However, we acknowledge that papyrus, along with the environmental conditions during our measurements, may not be broadly representative of typical C₄ species. Future work should aim to include a wider range of species and ideally those that are ecologically abundant and physiologically representative of the C₃ and C₄ photosynthetic pathways.

We furthermore recommend to perform experiments under environmental conditions closer to natural field conditions, in particular using higher PAR than in our experiments. However, measuring at high PAR in a plant chamber, while maintaining a sufficient COS mole fraction difference between in- and outgoing air to quantify COS isotope discrimination may introduce technical challenges, especially related to water condensation on chamber walls and sampling lines, which will need to be overcome.

Aditionally, the influence of soil water availability, VPD, and nutrient availability on COS isotope discrimination remains unexplored. Investigating these environmental variables may yield insights into mesophyll conductance and its influence on the LRU.

Finally, we recommend future studies to directly measure the isotope discrimination occuring during the CAcatalyzed hydrolysis of COS. Precisely quantifying the CA discrimination factor, h, as defined in Eq. (4), would provide a critical constraint on possible values for total observed isotope discrimination across different plant species. This would be beneficial for upscaling the isotope signatures to the global scale. Furthermore, better constraining h would enable more accurate estimations of CA activity, thereby improving our understanding of the physiological processes underlying plant COS assimilation. Deleted: does not require ligh

Deleted: t.

Deleted: indicating some

Deleted: did show a

Deleted: However, C_i^S / C_a^S and C_m^S / C_a^S were also not different between our measured C_3 and C_4 species, hence similar isotope discrimination is expected.

860 Appendices

Appendix A: Supplementary figures

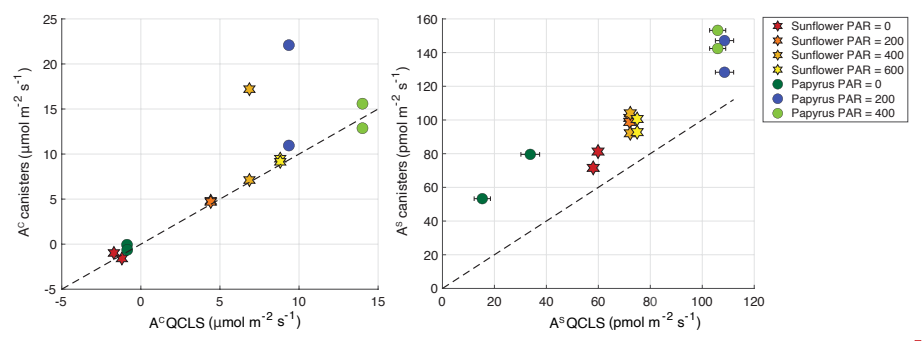
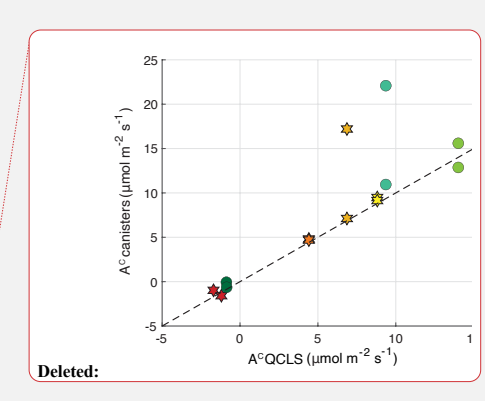


Figure A1. CO₂ and COS fluxes in µmol m⁻² s⁻¹ and pmol m⁻² s⁻¹, respectively, calculated from the discrete samples that were analyzed on the mass spectrometer, plotted against the fluxes that were calculated from the online QCLS measurements. Uncertainty bars are ± 1a, obtained using error propagation of the measurement errors on all the components used during the flux calculations (see supplementary materials). The errors are only depicted when they are larger than the symbols. The stars symbols are the sunflower data, and the circles are the papyrus data. The different color shadings indicate the varying PAR levels in µmol m⁻² s⁻¹. The black dashed line shows the one-to-one line, for reference. The two samples that clearly fall off the line in the CO₂ plot were excluded from both the CO₂ and COS dataset, as these sample canisters had possibly leaked or were contaminated with air other than the plant chamber air.



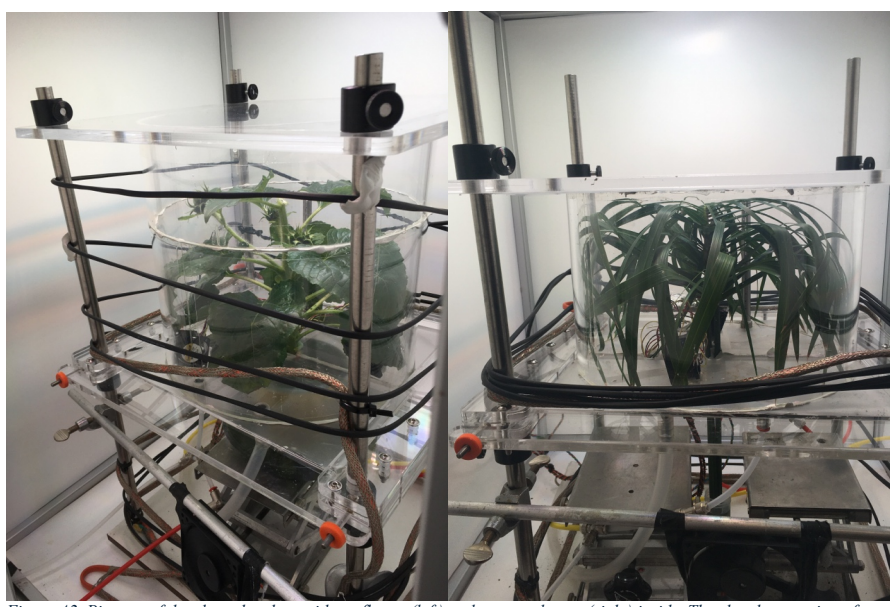


Figure 42. Pictures of the plant chamber, with sunflower (left) and papyrus leaves (right) inside. The chamber consists of two cylinders, connected to each other and to the upper and lower panels with Terostat RB VII. The plant pot and soil are kept outside of the chamber and the chamber is sealed onto the stem with Terostat as well. The black wires are automated (computer controlled) heating wires, ensuring constant temperature around the chamber.

Appendix B: Gas exchange calculations for CO2 and COS

We detail gas exchange equations of von Caemmerer and Farquhar (1981) for CO_2 and adapt this theory to derive gas exchange parameters for COS. For assimilation rates and mixing ratios we adopt a nomenclature where the superscript c refers to CO_2 and s to COS. For conductances the subscript represents the molecule of interest (w – water, c – CO_2 , s – COS) and the superscript the type of conductance (t – total, b – boundary layer, s – stomata).

CO2 and COS assimilation rates (Ac, As, µmol CO2 m-2 s-1, As given by Eq. (5)):

885
$$A^{c} = \frac{u_{e}}{S} \left(c_{e}^{c} - c_{a}^{c} \frac{1 - w_{e}}{1 - w_{a}} \right), \tag{B1}$$
where u_{e} is the molar flow of air entering the chamber (mol air s⁻¹), S is the leaf area (m²), c_{e}^{c} and c_{a}^{c} (μ mol CO₂ mol

where u_e is the molar flow of air entering the chamber (mol air s⁻¹), S' is the leaf area (m²), c_e^c and c_a^c (µmol CO₂ mol air⁻¹) are the [CO₂] in the air entering and leaving the chamber, respectively, and c_e^s and c_a^s (pmol COS mol air⁻¹) are the [COS] in the air entering and leaving the chamber, respectively.

 $\underline{Transpiration\;rate}\;(mol\;H_2O\;m^{\text{-}2}s^{\text{-}1})$

875

895

$$E = \frac{u_e}{S} \frac{w_a - w_e}{1 - w_a},$$
 (B2)

where w_e , w_a (mol of H₂O mol air⁻¹) are the mole fractions of water vapor in the air *entering* the chamber and in the chamber *air* (which equals to the air *out* of the chamber)

<u>Total conductance to water vapor</u> (g_w^t , mol H₂O m² s⁻¹):

$$g_w^t = E \frac{1 - \frac{w_i + w_a}{2}}{w_i - w_a},\tag{B3}$$

Deleted:

Deleted: 3

Deleted:

$$w_i = \frac{0.61635e^{\frac{17.502T_l}{240.97+T_l}}}{P_a},\tag{B4}$$

where P_a (kPa) is atmosphere pressure in the chamber.

Stomata conductance to water (g_s^w , mol H₂O m⁻² s⁻¹) is:

905

910

920

925

$$g_s^w = \frac{1}{\frac{1}{g_t^w} - \frac{1}{g_b^w}}, \tag{B5}$$
 where g_b^w is the boundary layer conductance to water, a characteristic of each plant chamber, but often very large in

well stirred chambers (a requisite for gas exchange).

Total conductance to CO₂ (g_t^c , mol CO₂ m⁻² s⁻¹) and COS (g_t^s , mol COS m⁻² s⁻¹):

 $g_t^c = \frac{1}{\frac{1.6}{g_s^w} + \frac{1.37}{g_s^w}},$

$$\frac{g_s^w + g_b^w}{g_b^w}$$

 $g_t^s = \frac{1}{\frac{1.94}{g_s^w} + \frac{1.56}{g_p^w}},$ (B7)

where the coefficient 1.6 and 1.37 (mol H₂O mol CO₂-1) are the ratio of diffusivities of CO₂ to water vapor in air, and in the boundary layer, respectively. The coefficients 1.94 and 1.56 (mol H₂O mol COS⁻¹) are the ratio of diffusivities of COS to water vapor in air, and boundary layer, respectively (Fuller et al., 1966; Farquhar & Lloyd, 1993).

915 Concentration inside the leaf of CO_2 (c_i^c , μ mol CO_2 mol wet air⁻¹) and COS (c_i^s , μ mol COS mol wet air⁻¹)

 A^c and A^s are determined with gas exchange with Eqs. (B1) and (\mathfrak{J}), and can also be related to the [CO₂] and [COS] inside the leaf with the equations:

$$A^{c} = g_{t}^{c}(c_{a}^{c} - c_{i}^{c}) - E\frac{c_{a}^{c} + c_{i}^{c}}{2},$$
(B8)

$$A^{s} = g_{t}^{s} (c_{a}^{s} - c_{t}^{s}) - E \frac{c_{a}^{s} + c_{t}^{s}}{2}, \tag{B9}$$

where $E \frac{c_n^c + c_i^c}{2}$ and $E \frac{c_n^2 + c_i^c}{2}$ are ternary corrections that accounts for the influence of transpiration on the diffusion of CO₂ and COS into the leaf. Solving c_i^c from Eqn 9 and c_i^s from Eq. (B2) results in:

$$c_i^c = \frac{\left(g_t^c - \frac{E}{2}\right)c_a^c - A^c}{g_t^c + \frac{E}{2}},\tag{B10}$$

$$c_{i}^{s} = \frac{\left(g_{t}^{s} - \frac{E}{2}\right)c_{a}^{s} - A^{s}}{g_{t}^{s} + \frac{E}{2}}.$$
(B11)

COS concentration in the mesophyll at the sites of CA (c_m^s , pmol COS mol wet air⁻¹):

By analogy with the model for photosynthetic discrimination against ¹³CO₂ (Farquhar et al., 1982; Farquhar & Cernusak, 2012) discrimination against CO³⁶S (‰) during plant uptake can be described:

$$\Delta^{34}S = \frac{1}{1-t} \frac{c_a^s - c_i^s}{c_a^s} + \frac{1+t}{1-t} \left[a_m \frac{c_i^s - c_m^s}{c_a^s} + h \frac{c_m^s}{c_a^s} \right], \tag{B12}$$

Deleted: 5

Deleted: 6

Deleted: 7

(B6)

Deleted: 8

Deleted: B2

Deleted: 9

Deleted: 10

Deleted: 10

Deleted: 1

Deleted: 2

where $a_{\overline{c}^{S}}$ (‰) is the weighted discrimination for diffusion across the leaf boundary layer and inside the mesophyll, calculated as:

$$a_{c_i^s} = \frac{a_b(c_a^s - c_s^s) + a_s(c_s^s - c_i^s)}{c_a^s - c_i^s},$$
(B13)

with c_s^s , the [COS] (pmol COS mol wet air⁻¹) at the leaf surface, is:

 $c_s^s = c_a^s - A^s \frac{1.56}{g_h^w}.$ (B14)

945

950

955

The t is a ternary correction factor calculated as (Farquhar & Cernusak, 2012):

$$t = \alpha_{ac} \frac{E}{2g_t^s},\tag{B15}$$

where $\alpha_{ac} = 1 + \frac{\alpha_{cl}}{1000}$

The a_b (= 3.5%), a_s (= 5.2%), and a_m (= 0.5%) are fractionations for COS diffusion across the boundary layer, across the stomata, and due to COS dissolution and diffusion in water through the mesophyll, respectively (Davidson et al., 2022). h (=15 ± 2‰) is the fractionation during COS hydrolysis by CA (Davidson et al., 2022).

The c_m^s can be solved from Eqn 13 as:

$$c_{m}^{s} = \frac{(1-t) \cdot \Delta^{34} S \cdot c_{a}^{s} - \alpha_{\overline{c_{i}^{s}}}(c_{a}^{s} - c_{i}^{s}) - (1+t) \cdot a_{m} \cdot c_{i}^{s}}{(1+t)(h-a_{m})}.$$
(B16)

Because $t \cong 0$, then Eq. (B1 \bigcirc) can be simplified to

$$c_m^s \cong \frac{\Delta^{34} \mathbf{S} \cdot c_a^s - a_{\overline{c_i^s}}(c_a^s - c_i^s) - a_m \cdot c_i^s}{h - a_m}. \tag{B17}$$

Substituting in Eq. (B17) the $a_{\overline{c_1}}$ for its expression given in Eq. (B14) and rearranging terms result in:

$$c_m^s \cong \frac{c_a^s(\Delta^{34}S - a_b) + c_s^s(a_b - a_s) + c_i^s(a_s - a_m)}{h - a_m}$$
(B18)

Substituting in Eq. (B18) the fractionation factors by their values results in:

$$c_m^s \cong \frac{(\Delta^{34} S - 3.5) c_s^s - 1.7 c_s^s + 4.7 c_i^s}{14.5}, \tag{B19}$$
 where $\Delta^{34} S$ (%) can be experimentally determined during measurements of gas exchange as (Evans *et al.*, 1986):

960

$$\Delta^{34}S = \frac{c_e^s}{c_e^s - c_a^s} \frac{\delta_a^{34} - \delta_e^{34}}{1 + \delta_a^{34} - \frac{c_e^s}{c^s - c^s}} (\delta_a^{34} - \delta_e^{34}), \tag{B20}$$

where c_e^s and c_e^s are the mole of COS in mole of dry air in the air *entering* and going *out* the chamber, and δ_e^{34} and δ_e^{34} (per mil) are the δ_e^{34} S isotope composition of the air entering and leaving the chamber, respectively. The term $c_e^s = c_e^s = c_$

 $\delta_a^{34} = 10\%$, then 0.0010 should be used).

We present c_m^s values calculated including ternary (Eq. (B1 \odot). Ignoring ternary overestimated $c_m^s \sim 1\%$ at PAR = 200 and $\sim 5\%$ at PAR = 600.

970

Appendix C: Overview of CO34S plant isotope discrimination data

Deleted: 4

Deleted: 5

Deleted: 6

Deleted: 7

Deleted: 7

Deleted: S

Deleted: 8

Deleted: 8

Deleted: 9

Deleted: 9

Deleted: S

Deleted: 20

Formatted: English (US)

Deleted: cos

Deleted: 0 Deleted: 0

Deleted: 0

Deleted: 0

Deleted: 1

Deleted: δ_0^{34}

Publication	Plant species	[COS] (nmol	[CO ₂] (µmol	PAR (μmol m ⁻²	<u>34∆</u>	<u>LRU</u>
		<u>mol⁻¹)</u>	<u>mol⁻¹)</u>	<u>s-1</u>)	(‰ <u>)</u>	
Davidson et al.	<u>Scindapsus</u>	0.53 ± 0.02	<u>500 ± 80</u>	<u>15.7</u>	1.6 ±	<u>0.7 ±</u>
(2022)	aureus (C ₃)				0.1	<u>0.1</u>
Davidson et al.	Zea mayz	0.53 ± 0.02	<u>500 ± 80</u>	15.7	5.4 ±	1.7 ±
(2022)					0.5	0.3
Davidson et al.	Scindapsus	3.4 ± 0.1	$\underline{2900 \pm 90}$	<u>15.7</u>	4.9 ±	2.4 ±
(2022)	aureus (C3)				0.5	0.3
Davidson et al.	Zea mayz (C ₄)	3.4 ± 0.1	2900 ± 90	<u>15.7</u>	9.2 ±	<u>1.0</u> ±
(2022)					0.4	<u>0.1</u>
Baartman et al	<u>Helianthus</u>	2.2 ± 0.02	<u>434 ± 1</u>	<u>200</u>	3.6 ±	<u>5.2</u> ±
(this study)	annuus (C3)				1.2	<u>0.16</u>
Baartman et al	<u>Helianthus</u>	2.2 ± 0.02	<u>434 ± 1</u>	<u>400</u>	3.7 ±	3.1 ±
(this study)	annuus (C3)				0.4*	<u>0.11</u>
Baartman et al	<u>Helianthus</u>	2.2 ± 0.02	434 ± 1	<u>600</u>	2.8 ±	2.3 ±
(this study)	annuus (C3)				0.6	0.08
Baartman et al	Helianthus	2.2 ± 0.02	<u>434 ± 1</u>	0	4.7 ±	Ξ
(this study)	annuus (C3)				0.4*	
Baartman et al	<u>Helianthus</u>	2.2 ± 0.02	<u>434 ± 1</u>	0	1.3 ±	Ξ
(this study)	annuus (C3)				0.4*	
Baartman et al	<u>Cyperus</u>	2.4 ± 0.04	427 ± 0.5	200	2.5 ±	3.0 ±
(this study)	papyrus (C ₄)				0.4*	0.11
Baartman et al	<u>Cyperus</u>	2.4 ± 0.04	427 ± 0.5	<u>400</u>	2.6 ±	<u>1.7 ±</u>
(this study)	papyrus (C ₄)				0.4	0.06

Formatted: Not Superscript/ Subscript
Formatted Table
Formatted: English (US)
Formatted: English (US)

Formatted: Left

Formatted: Font: Italic

Formatted: Font: Not Bold

Data availability

995 The dataset is available at: 10.5281/zenodo.14677494

Author contribution

1000

Conceptualization: SLB, MCK, MEP, LW. Data curation: SLB. Formal analysis: SLB, NUL. Funding acquisition: MCK. Investigation: SLB, SMD, MW, LMJK, LM, AC, SH. Methodology: SLB, SMD, MW, LMJK, MEP. Resources: SMD, MW, LM, SH. Supervision: MEP, TR, MCK. Visualization: SLB, NUL. Writing – original draft preparation: SLB, NUL. Writing – review & editing: SMD, MW, LMJK, NUL, LM, MEP, AC, LW, TR, SH, MCK.

*n = 1, error states is the single measurement precision instead of the repeatability precision

Competing interests

The authors declare that they have no conflict of interest

1005

Acknowledgements

We are grateful for the technical support from Carina van der Veen, Marcel Portanger and Giorgio Cover. The authors gratefully acknowledge the insightful discussions with Jérôme Ogée.

1010 Financial support

This project has received funding from the European Research Council (ERC) under the European Union's Horizon 2020 research and innovation program under grant agreement No 742798 (COS-OCS; to M. C. Krol)

References

1015

- Adnew, G. A., Pons, T. L., Koren, G., Peters, W., & Röckmann, T. (2020). Leaf-scale quantification of the effect of photosynthetic gas exchange on Δ 17 O of atmospheric CO 2. *Biogeosciences*, 17(14), 3903-3922.
- Angert, A., Said-Ahmad, W., Davidson, C., & Amrani, A. (2019). Sulfur isotopes ratio of atmospheric carbonyl sulfide constrains its sources. *Scientific reports*, 9(1), 741.
 - Asaf, D., Rotenberg, E., Tatarinov, F., Dicken, U., Montzka, S. A., and Yakir, D. (2013). Ecosystem photosynthesis inferred from measurements of carbonyl sulphide flux. Nature Geoscience, 6(3):186–190.
- 1025 Aubrey, D. P., & Teskey, R. O. (2009). Root-derived CO2 efflux via xylem stream rivals soil CO2 efflux. New Phytologist, 184(1), 35-40.
- Baartman, S. L., Krol, M. C., Röckmann, T., Hattori, S., Kamezaki, K., Yoshida, N., & Popa, M. E. (2021). A GC-IRMS method for measuring sulfur isotope ratios of carbonyl sulfide from small air samples. *Open Research*1030 Europe, 1.

Belviso, S., Abadie, C., Montagne, D., Hadjar, D., Tropée, D., Vialettes, L., Kazan, V., Delmotte, M., Maignan, F., Remaud, M., Ramonet, M., Lopez, M., Yver-Kwok C. & Ciais, P. (2022). Carbonyl sulfide (COS) emissions in two agroecosystems in central France. *PLoS One*, *17*(12), e0278584.

1035

Berkelhammer, M., Alsip, B., Matamala, R., Cook, D., Whelan, M. E., Joo, E., ... & Meyers, T. (2020). Seasonal evolution of canopy stomatal conductance for a prairie and maize field in the midwestern United States from continuous carbonyl sulfide fluxes. *Geophysical Research Letters*, 47(6), e2019GL085652.

- Billesbach, D. P., Berry, J. A., Seibt, U., Maseyk, K., Torn, M. S., Fischer, M. L., ... & Campbell, J. E. (2014). Growing season eddy covariance measurements of carbonyl sulfide and CO2 fluxes: COS and CO2 relationships in Southern Great Plains winter wheat. Agricultural and Forest Meteorology, 184, 48-55.
- Bloemen, J., McGuire, M. A., Aubrey, D. P., Teskey, R. O., & Steppe, K. (2013). Transport of root-respired CO2 via the transpiration stream affects aboveground carbon assimilation and CO2 efflux in trees. *New Phytologist*, 197(2), 555-565.
- Brenninkmeijer, C. A. M.: Measurement of the abundance of 14CO in the atmosphere and the 13C / 12C and 18O/16O ratio of atmospheric CO with applications in New Zealand and Antarctica, J. Geophys. Res., 98, 10595–10614, doi:10.1029/93JD00587, 1993.

Buck, A. L. (1981). New equations for computing vapor pressure and enhancement factor. *Journal of Applied Meteorology* (1962-1982), 1527-1532.

Formatted: Font: 10 pt
Formatted: Font: 10 pt

Formatted: Font: 10 pt

1055	von Caemmerer, S. V., & Farquhar, G. D. (1981). Some relationships between the biochemistry of photosynthesis and the gas exchange of leaves. <i>Planta</i> , <i>153</i> , 376-387.	
	Campbell, J. E., Carmichael, G. R., Chai, T., Mena-Carrasco, M., Tang, Y., Blake, D. R., & Stanier, C. O. (2008). Photosynthetic control of atmospheric carbonyl sulfide during the growing season. <i>Science</i> , 322(5904), 1085-1088.	Formatted: Font: 10 pt
1060	Cerling, T. E., Harris, J. M., MacFadden, B. J., Leakey, M. G., Quade, J., Eisenmann, V., & Ehleringer, J. R. (1997). Global vegetation change through the Miocene/Pliocene boundary. <i>Nature</i> , <i>389</i> (6647), 153-158.	
1065	Cernusak, L. A., Ubierna, N., Jenkins, M. W., Garrity, S. R., Rahn, T., Powers, H. H., & Farquhar, G. D. (2018). Unsaturation of vapour pressure inside leaves of two conifer species. <i>Scientific reports</i> , 8(1), 1-7.	Formatted: Font: 10 pt
1 070	Cernusak, L. A., Ubierna, N., Winter, K., Holtum, J. A., Marshall, J. D., & Farquhar, G. D. (2013). Environmental and physiological determinants of carbon isotope discrimination in terrestrial plants. <i>New Phytologist</i> , 200(4), 950-965.	
1070	Cernusak, L. A., Wong, S. C., Stuart-Williams, H., Márquez, D. A., Pontarin, N., & Farquhar, G. D. (2024). Unsaturation in the air spaces of leaves and its implications. <i>Plant, Cell & Environment</i> , 47(10), 3685-3698.	Formatted: Font: 10 pt
1075	Cho, A., Kooijmans, L. M., Kohonen, K. M., Wehr, R., & Krol, M. C. (2023). Optimizing the carbonic anhydrase temperature response and stomatal conductance of carbonyl sulfide leaf uptake in the Simple Biosphere model (SiB4). <i>Biogeosciences</i> , 20(13), 2573-2594.	
1080	Commane, R., Meredith, L. K., Baker, I. T., Berry, J. A., Munger, J. W., Montzka, S. A., & Wofsy, S. C. (2015). Seasonal fluxes of carbonyl sulfide in a midlatitude forest. <i>Proceedings of the National Academy of Sciences</i> , 112(46), 14162-14167.	
	Davidson, C., Amrani, A., & Angert, A. (2021). Tropospheric carbonyl sulfide mass balance based on direct measurements of sulfur isotopes. <i>Proceedings of the National Academy of Sciences</i> , 118(6), e2020060118.	
1085	Davidson, C., Amrani, A., and Angert, A. (2022). Carbonyl sulfide sulfur isotope fractionation during uptake by C3 and C4 plants. Journal of Geophysical Research: Biogeosciences, 127(10):e2022JG007035.	
1090	Eggels, S., Blankenagel, S., Schön, C. C., & Avramova, V. (2021). The carbon isotopic signature of C4 crops and its applicability in breeding for climate resilience. <i>Theoretical and Applied Genetics</i> , 134(6), 1663-1675.	
1090	Ellsworth, P. Z., & Cousins, A. B. (2016). Carbon isotopes and water use efficiency in C4 plants. <i>Current Opinion in Plant Biology</i> , 31, 155-161.	
1095	Evans, J. R., Sharkey, T. D., Berry, J. A., & Farquhar, G. D. (1986). Carbon isotope discrimination measured concurrently with gas exchange to investigate CO2 diffusion in leaves of higher plants. <i>Functional Plant Biology</i> , 13(2), 281-292.	
1100	Farquhar, G. D. (1983). On the nature of carbon isotope discrimination in C4 species. <i>Functional Plant Biology</i> , 10(2), 205-226.	
1100	Farquhar, G. D., von Caemmerer, S. V., & Berry, J. A. (1980). A biochemical model of photosynthetic CO ₂ assimilation in leaves of C 3 species. <i>planta</i> , 149, 78-90.	
1105	Farquhar, G. D., & Cernusak, L. A. (2012). Ternary effects on the gas exchange of isotopologues of carbon dioxide. <i>Plant, Cell & Environment</i> , 35(7), 1221-1231.	
	Farquhar, G. D., Ehleringer, J. R., & Hubick, K. T. (1989). Carbon isotope discrimination and photosynthesis. <i>Annual review of plant physiology and plant molecular biology</i> , 40(1), 503-537.	

1110	Farquhar, G. D., O'Leary, M. H., & Berry, J. A. (1982). On the relationship between carbon isotope discrimination and the intercellular carbon dioxide concentration in leaves. <i>Functional Plant Biology</i> , 9(2), 121-137.	
1115	Farquhar, G. D., & Lloyd, J. (1993). Carbon and oxygen isotope effects in the exchange of carbon dioxide between terrestrial plants and the atmosphere. In <i>Stable isotopes and plant carbon-water relations</i> (pp. 47-70). Academic Press.	
I	Farquhar, G. D., Lloyd, J., Taylor, J. A., Flanagan, L. B., Syvertsen, J. P., Hubick, K. T., & Ehleringer, J. R. (1993). Vegetation effects on the isotope composition of oxygen in atmospheric CO2. <i>Nature</i> , 363(6428), 439-443.	Formatted: Font: 11 pt
1120	Farquhar, G. D., & Richards, R. A. (1984). Isotopic composition of plant carbon correlates with water-use efficiency of wheat genotypes. <i>Functional Plant Biology</i> , 11(6), 539-552.	Formatted: Font: 10 pt
ı	Francey, R. J. and Tans, P. P.: Latitudinal variation in oxygen-18 of atmospheric CO2, Nature, 327, 2 pp., 1987.	
1125	Friedlingstein, P., O'Sullivan, M., Jones, M. W., Andrew, R. M., Bakker, D. C., Hauck, J., Le Quéré, C., Peters, G. P., Peters, W., Pongratz, J., Sitch, S., Canadell, J. G., Ciais, P., Jackson, R. B., Alin, S. R., Anthoni, P., Bates, N. R., Becker M., Bellouin, N., & Zheng, B. (2023). Global carbon budget 2023. Earth System Science Data, 15(12), 5301-5369, doi: 10.5194/essd-15-5301-2023,	(Frank J.F. L. I (IV)
1130		Formatted: English (UK)
1130	Fuller, E. N., Schettler, P. D., & Giddings, J. C. (1966). New method for prediction of binary gas-phase diffusion coefficients. <i>Industrial & Engineering Chemistry</i> , 58(5), 18-27.	
1135	Gillon, J. S., & Yakir, D. (2000). Naturally low carbonic anhydrase activity in C4 and C3 plants limits discrimination against C18OO during photosynthesis. <i>Plant, Cell & Environment</i> , 23(9), 903-915.	
1100	Gentsch, L., Sturm, P., Hammerle, A., Siegwolf, R., Wingate, L., Ogée, J., & Knohl, A. (2014). Carbon isotope discrimination during branch photosynthesis of Fagus sylvatica: field measurements using laser spectrometry. <i>Journal of experimental botany</i> , 65(6), 1481-1496.	
1140	Goldan, P. D., Fall, R., Kuster, W. C., & Fehsenfeld, F. C. (1988). Uptake of COS by growing vegetation: A major tropospheric sink. <i>Journal of Geophysical Research: Atmospheres</i> , 93(D11), 14186-14192.	Formatted: Font: 10 pt
	Howard, A. R., & Donovan, L. A. (2007). Helianthus nighttime conductance and transpiration respond to soil water	Formatted: Font: 10 pt
1145	but not nutrient availability. Plant Physiology, 143(1), 145-155.	
	Kesselmeier, J., & Merk, L. (1993). Exchange of carbonyl sulfide (COS) between agricultural plants and the atmosphere: Studies on the deposition of COS to peas, corn and rapeseed. <i>Biogeochemistry</i> , 23, 47-59.	Formatted: Font: 10 pt
1150	Kohn, M. J. (2010). Carbon isotope compositions of terrestrial C3 plants as indicators of (paleo) ecology and (paleo) climate. <i>Proceedings of the National Academy of Sciences</i> , 107(46), 19691-19695.	
1155	Kooijmans, L. M., Maseyk, K., Seibt, U., Sun, W., Vesala, T., Mammarella, I., Kolari, P., Aalto, J., Franchin, A., Vecchi, R., et al. (2017). Canopy uptake dominates nighttime carbonyl sulfide fluxes in a boreal forest. Atmospheric Chemistry and Physics, 17(18):11453–11465.	
1133	Kooijmans, L. M., Sun, W., Aalto, J., Erkkilä, K.M., Maseyk, K., Seibt, U., Vesala, T., Mammarella, I., and Chen, H. (2019). Influences of light and humidity on carbonyl sulfide-based estimates of photosynthesis. Proceedings of the National Academy of Sciences, 116(7):2470–2475.	
1160	Kromdijk, J., Griffiths, H., & Schepers, H. E. (2010). Can the progressive increase of C4 bundle sheath leakiness at low PFD be explained by incomplete suppression of photorespiration? <i>Plant, cell & environment</i> , <i>33</i> (11), 1935-1948.	
1165	Kubásek, J., Urban, O., & Šantrůček, J. (2013). C4 plants use fluctuating light less efficiently than do C3 plants: a study of growth, photosynthesis and carbon isotope discrimination. <i>Physiologia plantarum</i> , <i>149</i> (4), 528-539.	

	Kuhn, U., & Kesselmeier, J. (2000). Environmental variables controlling the uptake of carbonyl sulfide by lichens. Journal of Geophysical Research: Atmospheres, 105(D22), 26783-26792.	Formatted: Font: 10 pt
1170	Lazzarin, M., Dupont, K., van Ieperen, W., Marcelis, L. F., & Driever, S. M. (2024). Far-red light effects on plant photosynthesis: from short-term enhancements to long-term effects of artificial solar light. <i>Annals of Botany</i> , mcae104.	
1175	Lai, J., Kooijmans, L. M., Sun, W., Lombardozzi, D., Campbell, J. E., Gu, L., & Sun, Y. (2024). Terrestrial photosynthesis inferred from plant carbonyl sulfide uptake. <i>Nature</i> , 1-7.	
	Li, M., & Jones, M. B. (1995). CO2 and O2 transport in the aerenchyma of Cyperus papyrus L. <i>Aquatic Botany</i> , 52(1-2), 93-106.	
1180	Maignan, F., Abadie, C., Remaud, M., Kooijmans, L. M., Kohonen, K. M., Commane, R., & Peylin, P. (2021). Carbonyl sulfide: comparing a mechanistic representation of the vegetation uptake in a land surface model and the leaf relative uptake approach. <i>Biogeosciences</i> , 18(9), 2917-2955.	
		Formatted: Font: 10 pt
1185	Maseyk, K., Berry, J. A., Billesbach, D., Campbell, J. E., Torn, M. S., Zahniser, M., & Seibt, U. (2014). Sources and sinks of carbonyl sulfide in an agricultural field in the Southern Great Plains. <i>Proceedings of the National Academy of Sciences</i> , 111(25), 9064-9069.	
	Miner, G. L., & Bauerle, W. L. (2017). Seasonal variability of the parameters of the Ball–Berry model of stomatal conductance in maize (Zea mays L.) and sunflower (Helianthus annuus L.) under well-watered and water-stressed	Formatted: Font: 10 pt
1190	conditions. <i>Plant, cell & environment, 40</i> (9), 1874-1886.	
	Montzka, S. A., Calvert, P., Hall, B. D., Elkins, J. W., Conway, T. J., Tans, P. P., & Sweeney, C. (2007). On the global distribution, seasonality, and budget of atmospheric carbonyl sulfide (COS) and some similarities to CO2.	Formatted: Font: 10 pt
 1195	Journal of Geophysical Research: Atmospheres, 112(D9).	
	Pengelly, J. J., Sirault, X. R., Tazoe, Y., Evans, J. R., Furbank, R. T., & Von Caemmerer, S. (2010). Growth of the C4 dicot Flaveria bidentis: photosynthetic acclimation to low light through shifts in leaf anatomy and biochemistry. <i>Journal of experimental botany</i> , 61(14), 4109-4122.	
1200	Plowman, A. B. (1906). The comparative anatomy and phylogeny of the Cyperaceae. <i>Annals of Botany</i> , 20(77), 1-33.	
1205	Protoschill-Krebs, G., & Kesselmeier, J. (1992). Enzymatic pathways for the consumption of carbonyl sulphide (COS) by higher plants. <i>Botanica Acta</i> , 105(3), 206-212.	
1203	Protoschill-Krebs, G., Wilhelm, C., & Kesselmeier, J. (1996). Consumption of carbonyl sulphide (COS) by higher plant carbonic anhydrase (CA). <i>Atmospheric Environment</i> , 30(18), 3151-3156.	
	Sandoval-Soto, L., Stanimirov, M., Von Hobe, M., Schmitt, V., Valdes, J., Wild, A., & Kesselmeier, J. (2005).	Formatted: Font: 10 pt
1210	Global uptake of carbonyl sulfide (COS) by terrestrial vegetation: Estimates corrected by deposition velocities normalized to the uptake of carbon dioxide (CO 2). <i>Biogeosciences</i> , 2(2), 125-132.	(
1215	Seibt, U., Wingate, L., Berry, J. A., & Lloyd, J. (2006). Non-steady state effects in diurnal 18O discrimination by Picea sitchensis branches in the field. <i>Plant, Cell & Environment</i> , 29(5), 928-939.	
1213	Spielmann, F. M., Hammerle, A., Kitz, F., Gerdel, K., Alberti, G., Peressotti, A., & Wohlfahrt, G. (2023). On the variability of the leaf relative uptake rate of carbonyl sulfide compared to carbon dioxide: Insights from a paired field study with two soybean varieties. <i>Agricultural and Forest Meteorology</i> , 338, 109504.	
1220	Stimler, K., Berry, J. A., Montzka, S. A., and Yakir, D. (2011). Association between carbonyl sulfide uptake and 18Δ during gas exchange in C3 and C4 leaves. Plant physiology, $157(1):509\ 517$.	
	29	
	2)	

Stimler, K., Berry, J. A., & Yakir, D. (2012). Effects of carbonyl sulfide and carbonic anhydrase on stomatal conductance. *Plant Physiology*, *158*(1), 524-530.

1225
Sun, W., Berry, J. A., Yakir, D., & Seibt, U. (2022). Leaf relative uptake of carbonyl sulfide to CO2 seen through the lens of stomatal conductance–photosynthesis coupling. *New Phytologist*, 235(5), 1729-1742.

Sun, W., Maseyk, K., Lett, C., & Seibt, U. (2024). Restricted internal diffusion weakens transpiration—photosynthesis coupling during heatwaves: Evidence from leaf carbonyl sulphide exchange. *Plant, Cell & Environment*, 47(5), 1813-1833.

Tezara, W., Driscoll, S., & Lawlor, D. W. (2008). Partitioning of photosynthetic electron flow between CO₂ assimilation and O₂ reduction in sunflower plants under water deficit. *Photosynthetica*, 46, 127-134.

Ubierna, N., Sun, W. E. I., Kramer, D. M., & Cousins, A. B. (2013). The efficiency of C4 photosynthesis under low light conditions in Zea mays, Miscanthus x giganteus and Flaveria bidentis. *Plant, cell & environment*, 36(2), 365-381

1240 Vesala, T., Kohonen, K. M., Kooijmans, L. M., Praplan, A. P., Foltýnová, L., Kolari, P., ... & Mammarella, I. (2022). Long-term fluxes of carbonyl sulfide and their seasonality and interannual variability in a boreal forest. Atmospheric Chemistry and Physics, 22(4), 2569-2584.

Wehr, R., Commane, R., Munger, J. W., McManus, J. B., Nelson, D. D., Zahniser, M. S., Saleska, S. R., and Wofsy, S. C. (2017). Dynamics of canopy stomatal conductance, transpiration, and evaporation in a temperate deciduous forest, validated by carbonyl sulfide uptake. Biogeosciences, 14(2):389–401.

Wehr, R., & Saleska, S. R. (2015). An improved isotopic method for partitioning net ecosystem-atmosphere CO2 exchange. *Agricultural and Forest Meteorology*, 214, 515-531.

Whelan, M. E., Lennartz, S. T., Gimeno, T. E., Wehr, R., Wohlfahrt, G., Wang, Y., Kooijmans, L. M., Hilton, T. W., Belviso, S., Peylin, P., et al. (2018). Reviews and syntheses: Carbonyl sulfide as a multi-scale tracer for carbon and water cycles. Biogeosciences, 15(12):3625–3657.

Wingate, L., Ogée, J., Burlett, R., Bosc, A., Devaux, M., Grace, J., Loustau, D., and Gessler, A. (2010).

1255 Photosynthetic carbon isotope discrimination and its relationship to the carbon isotope signals of stem, soil and ecosystem respiration. New Phytologist, 188(2):576–589.

1250

1260

Wingate, L., Seibt, U., Moncrieff, J. B., Jarvis, P. G., & Lloyd, J. O. N. (2007). Variations in 13C discrimination during CO2 exchange by Picea sitchensis branches in the field. *Plant, Cell & Environment*, 30(5), 600-616.

Wohlfahrt, G., Brilli, F., Hörtnagl, L., Xu, X., Bingemer, H., Hansel, A., and Loreto, F. (2012). Carbonyl sulfide (COS) as a tracer for canopy photosynthesis, transpiration and stomatal conductance: potential and limitations. Plant, cell & environment, 35(4):657–667.

1265 Wohlfahrt, G., Hammerle, A., Spielmann, F. M., Kitz, F., & Yi, C. (2023). Novel estimates of the leaf relative uptake rate of carbonyl sulfide from optimality theory. *Biogeosciences*, 20(3), 589-596.

Yakir, D.: Oxygen-18 of leaf water: a crossroad for plant-associated isotopic signals, in: Stable isotopes: integration of biological, ecological and geochemical processes, edited by: Griffiths, H., BIOS Scientific Publishers, Oxford, 147–188, 1998.

Formatted: Font: 10 pt

Page 10: [1] Deleted	Baartman, Sophie	20/05/2025 10:54:00
Page 15: [2] Deleted	Baartman, Sophie	23/05/2025 14:59:00
Page 15: [2] Deleted	Baartman, Sophie	23/05/2025 14:59:00
Page 15: [2] Deleted	Baartman, Sophie	23/05/2025 14:59:00
Page 15: [2] Deleted	Baartman, Sophie	23/05/2025 14:59:00
Page 15: [3] Formatted	Baartman, Sophie	28/05/2025 20:19:00
Font: Not Bold	Daar unan, Sopme	26/03/2023 20.19.00
Page 15: [4] Formatted	Baartman, Sophie	16/06/2025 15:32:00
Font: Italic		
Page 15: [4] Formatted	Baartman, Sophie	16/06/2025 15:32:00
Font: Italic		
Page 15: [5] Formatted	Baartman, Sophie	26/05/2025 10:20:00
Not Superscript/ Subscript		
Page 15: [6] Formatted	Baartman, Sophie	02/06/2025 13:06:00
Font: Not Italic		
Page 15: [6] Formatted	Baartman, Sophie	02/06/2025 13:06:00
Font: Not Italic		
Page 15: [6] Formatted	Baartman, Sophie	02/06/2025 13:06:00
Font: Not Italic		
Page 15: [7] Formatted	Baartman, Sophie	28/05/2025 16:01:00
Not Superscript/ Subscript		
Page 15: [8] Formatted	Baartman, Sophie	02/06/2025 13:05:00
Not Superscript/ Subscript		
Page 15: [9] Formatted	Baartman, Sophie	02/06/2025 13:06:00
Font: Not Italic		
Page 15: [9] Formatted	Baartman, Sophie	02/06/2025 13:06:00
Font: Not Italic		
Page 15: [10] Formatted	Baartman, Sophie	28/05/2025 16:03:00
Not Superscript/ Subscript		
Page 15: [11] Formatted	Baartman, Sophie	02/06/2025 13:06:00
Superscript		
Page 15: [12] Formatted	Baartman, Sophie	28/05/2025 15:11:00
Font: 9 pt		
Page 15: [13] Formatted	Baartman, Sophie	28/05/2025 15:10:00
Left		
Page 15: [14] Formatted	Baartman, Sophie	28/05/2025 15:10:00
Left, Line spacing: single		
Page 15: [15] Formatted	Baartman, Sophie	28/05/2025 15:11:00
Font: 9 pt, Not Bold		

Page 15: [15] Formatted	Baartman, Sophie	28/05/2025 15:11:00
Font: 9 pt, Not Bold		
Page 15: [16] Formatted	Baartman, Sophie	28/05/2025 15:11:00
Font: 9 pt		
Page 15: [16] Formatted	Baartman, Sophie	28/05/2025 15:11:00
Font: 9 pt		
Page 15: [16] Formatted	Baartman, Sophie	28/05/2025 15:11:00
Font: 9 pt		
Page 15: [16] Formatted	Baartman, Sophie	28/05/2025 15:11:00
Font: 9 pt		
Page 15: [16] Formatted	Baartman, Sophie	28/05/2025 15:11:00
Font: 9 pt		
Page 15: [16] Formatted	Baartman, Sophie	28/05/2025 15:11:00
Font: 9 pt		
Page 15: [16] Formatted	Baartman, Sophie	28/05/2025 15:11:00
Font: 9 pt		
Page 15: [17] Formatted	Baartman, Sophie	28/05/2025 15:11:00
Font: 9 pt		
Page 15: [17] Formatted	Baartman, Sophie	28/05/2025 15:11:00
Font: 9 pt		
Page 15: [17] Formatted	Baartman, Sophie	28/05/2025 15:11:00
Font: 9 pt		
Page 15: [17] Formatted	Baartman, Sophie	28/05/2025 15:11:00
Font: 9 pt		